Free Radical Biology and Medicine 223 (2024) 384–397

Contents lists available at ScienceDirect

Free Radical Biology and Medicine

journal homepage: www.elsevier.com/locate/freeradbiomed

Harmonization of experimental procedures to assess mitochondrial respiration in human permeabilized skeletal muscle fibers☆

Carolina Doerrier [a,**], Pau Gama-Perez [b], Dominik Pesta [c,d,e,f,g], Giovanna Distefano [h], Stine D. Soendergaard [i], Karoline Maise Chroeis [i], Alba Gonzalez-Franquesa [j], Bret H. Goodpaster [h], Clara Prats [k,l], Marta Sales-Pardo [m], Roger Guimera [m,n], Paul M. Coen [h], Erich Gnaiger [a], Steen Larsen [i,o,***], Pablo M. Garcia-Roves [b,*]

[a] Oroboros Instruments, Schöpfstrasse 18, 6020, Innsbruck, Austria
[b] Dept Physiological Sciences, Univ Barcelona and Bellvitge Biomedical Research Inst, Spain
[c] Inst Clinical Diabetology, German Diabetes Center, Leibniz Center Diabetes Research Heinrich-Heine Univ Düsseldorf, Germany
[d] German Center Diabetes Research, Munich, Neuherberg, Germany
[e] Institute of Aerospace Medicine, German Aerospace Center (DLR), Cologne, Germany
[f] Center for Endocrinology, Diabetes and Preventive Medicine (CEDP), University Hospital Cologne, Cologne, Germany
[g] Cologne Excellence Cluster on Cellular Stress Responses in Aging-Associated Diseases (CECAD), Cologne, Germany
[h] Translational Research Institute AdventHealth, Orlando, FL, USA
[i] Xlab, Dept Biomedical Sciences, Center Healthy Aging, Fac Health Sciences, Denmark
[j] The Novo Nordisk Center Basic Metabolic Research, Section Integrative Physiology, Univ Copenhagen, Denmark
[k] Dept Biomedical Sciences, Center Healthy Aging, Fac Health Sciences, Denmark
[l] The Core Facility for Integrated Microscopy, Faculty of Health and Medical Sciences, University of Copenhagen, Denmark
[m] Dept of Chemical Engineering, Universitat Rovira I Virgili, Tarragona, Spain
[n] Institució Catalana de Recerca I Estudis Avançats (ICREA), Barcelona, Spain
[o] Clinical Research Centre, Medical University of Bialystok, Bialystok, Poland

ARTICLE INFO

Keywords:
Permeabilized skeletal muscle fibers
Mitochondrial respiration
High-resolution respirometry
Respiration medium MiR05
Respiration medium Z
O_2 regime
Blebbistatin

ABSTRACT

Aim: High-resolution respirometry in human permeabilized muscle fibers is extensively used for analysis of mitochondrial adaptions to nutrition and exercise interventions, and is linked to athletic performance. However, the lack of standardization of experimental conditions limits quantitative inter- and intra-laboratory comparisons.

Methods: In our study, an international team of investigators measured mitochondrial respiration of permeabilized muscle fibers obtained from three biopsies (*vastus lateralis*) from the same healthy volunteer to avoid inter-individual variability. High-resolution respirometry assays were performed together at the same laboratory to assess whether the heterogenity in published results are due to the effects of respiration media (MiR05 versus Z) with or without the myosin inhibitor blebbistatin at low- and high-oxygen regimes.

Results: Our findings reveal significant differences between respiration media for OXPHOS and ETcapacities supported by NADH&succinate-linked substrates at different oxygen concentrations. Respiratory capacities were approximately 1.5-fold higher in MiR05 at high-oxygen regimes compared to medium Z near air saturation. The presence or absence of blebbistatin in human permeabilized muscle fiber preparations was without effect on oxygen flux.

☆ This article is a contribution to the special issue entitled Unlocking Athletic Potential: Exploring Exercise Physiology from Mechanisms to Performance. Guest Edited by Maria Carmen Gomez Cabrera (University of Valencia, Spain) & Christoph Handschin (University of Basel, Switzerland).

* Corresponding author.
** Corresponding author.
*** Corresponding author. Xlab, Dept Biomedical Sciences, Center Healthy Aging, Fac Health Sciences, Denmark.
E-mail addresses: carolina.doerrier@gmail.com (C. Doerrier), p.gamaperez@gmail.com (P. Gama-Perez), Dominik.pesta@dlr.de (D. Pesta), Giovanna.Distefano@adventhealth.com (G. Distefano), wdz320@alumni.ku.dk (S.D. Soendergaard), rwn105@alumni.ku.dk (K.M. Chroeis), agonzalezfranquesa@gmail.com (A. Gonzalez-Franquesa), bret.goodpaster@adventhealth.com (B.H. Goodpaster), cprats@sund.ku.dk (C. Prats), marta.sales@urv.cat (M. Sales-Pardo), roger.guimera@urv.cat (R. Guimera), Paul.Coen@adventhealth.com (P.M. Coen), erich.gnaiger@oroboros.at (E. Gnaiger), stelar@sund.ku.dk (S. Larsen), pgarciaroves@ub.edu (P.M. Garcia-Roves).

https://doi.org/10.1016/j.freeradbiomed.2024.07.039
Received 5 April 2024; Received in revised form 11 July 2024; Accepted 29 July 2024
Available online 2 August 2024

Conclusion: Our study constitutes a basis to harmonize and establish optimum experimental conditions for respirometric studies of permeabilized human skeletal muscle fibers to improve reproducibility.

1. Introduction

Mitochondria are the major source of ATP production and reactive oxygen species in eukaryote cells. Mitochondria are also a nexus for anabolic and catabolic pathways, involved in key processes including autophagy and calcium handling, cellular stress response, and epigenetic reprogramming of the nuclear genome [1–4]. Athletes exercise to improve their aerobic fitness and/or skeletal muscle strength in order to achieve their competitive goals. It is important to understand adaptations to exercise practice for the optimization of athletes training programs. To this respect, there are a couple of recent review articles that summarize the molecular mechanisms causing acute [5] and exercise adaptations to endurance and strength training [6]. Training stimulates skeletal muscle mitochondrial biogenesis [7,8], and those adaptations are determinant of athletic performance [9]. It has been reported that both high intensity training [9] as well as moderate intensity training [7] improves mitochondrial content and function. In the same line, mitochondrial respiratory capacity could be ameliorated by both, endurance and resistance training programs [10,11]. Interestingly it seems as if excessive training causes impairments in mitochondrial respiratory capacity but not when normalized by mitochondrial content [12], even the interpretation of these results has been debated [13].

In addition, the importance of mitochondrial energetics for human health is underscored by a growing appreciation of its key involvement in pathophysiological conditions including aging and many age-related diseases such as cardiovascular diseases, cancer, and diabetes [14–17]. As such mitochondria are being increasingly considered as a target for the development of preventative and therapeutic strategies for human health, and anti-aging.

Mitochondria in skeletal muscle provide the necessary ATP to fuel contraction and maintain skeletal muscle metabolic health. Studies of muscle mitochondrial function have broadly focused on its role in athletic performance, aging, sarcopenia, and obesity/type 2 diabetes [18–22]. The importance of mitochondria in mediating the health benefits of exercise, caloric restriction, and some pharmacological therapeutics, including metformin has been investigated [10,23–26]. For this purpose, permeabilized muscle fibers (pfi) obtained from skeletal muscle biopsies are routinely used to assess mitochondrial function for diagnosis of mitochondrial diseases. Preparation of pfi offers tangible advantages over isolated mitochondria: (*1*) less tissue is required, (*2*) mitochondrial morphology is preserved, and (*3*) all mitochondrial populations are represented [27,28]. However, it is important to take into account that permeabilized muscle fibers have some limitations: (*1*) complexity of preparation and time-consuming nature, (*2*) heterogeneity, leading to more variability across experiments, (*3*) diffusion limitations, (*4*) inability to distinguish between mitochondrial sub-populations, and (*5*) incompatibility with certain methods. Although studies on human tissue biopsies are frequently statistically underpowered, they must consider the background effects of age, gender, sex, and environment [29]. As such, understanding the role of these key intrinsic aspects of human biology on the relationship between muscle mitochondrial energetics and human athletic performance or disease is paramount.

Analysis of previous publications identifies diverse experimental conditions among studies performed in human pfi. Thus we distinguish (*1*) experimental conditions (composition of respiration media; use of contraction inhibitors blebbistatin, Bleb, or N-benzyl-P-toluenesulfonamide, BTS; oxygen concentration range; experimental temperature), (*2*) experimental protocols using different substrate-uncoupler-inhibitor titration (SUIT) regimes addressing specific respiratory states, (*3*) preanalytical procedures (including fiber preparation), and (*4*) normalization of respiratory rate (for dry or wet mass of muscle fibers, mitochondrial markers). The influence of these factors must be considered when attempting to compare and combine datasets. Furthermore, sex [19,30,31], age [18–20,32–34], race [21], and physical fitness [8,9,35–50] are physiological factors that influence mitochondrial respiratory capacity. These variables and specific mitochondrial quality control criteria (such as cytochrome *c* control efficiency) must be considered when datasets are compared [22].

Table 1 reports data obtained from human studies (different gender, age, and physical fitness) conducted after the compilation performed by Gnaiger in 2009 [22]. The studies used various respiration media, presence/absence of contraction inhibitors, O_2 regimes, temperature, and normalization strategies. It is clear from data in Table 1 that respiratory rates are different, when different respiration media, O_2 regimes, or normalization strategies are used, and physical characteristics and health status differ of the participants investigated. A limitation to identify potential contributors to the variability observed in those data is the diversity of parameters present in study design and participants' characteristics. Therefore, a study that controls key experimental factors influencing respiratory capacities is necessary to separate the effects of methodological design from physiological variables.

The purpose of the present investigation is to explore the influence of the most widely used respiration media, the use of contraction inhibitors, and the O_2 concentration regime on respiratory capacities in human permeabilized skeletal muscle fibers, while excluding physiological variability between different donors.

2. Materials and methods

2.1. Biopsy donor and muscle biopsy

Three muscle biopsies were collected from a healthy, moderately-trained male (43 years old) on three consecutive days under identical conditions. The study was approved by the local ethics committee of Copenhagen and Frederiksberg in Denmark (hs:h-15002266). All procedures were carried out in accordance with the declaration of Helsinki. After an overnight fast a muscle biopsy was obtained at 9 a.m. from muscle *vastus lateralis* under local anesthesia (lidocaine; 5 mg/mL) using the Bergstrom needle modified for suction [51]. ~250 mg of muscle biopsy was immediately transferred to ice-cold biopsy preservation buffer (BIOPS, containing 2.77 mM CaK_2EGTA, 7.23 mM K_2EGTA, 20 mM imidazole, 20 mM taurine, 50 mM MES hydrate, 0.5 mM DTT, 6.56 mM $MgCl_2$, 5.77 mM ATP and 15 mM phosphocreatine; pH 7.1 on ice [52,53]. Each biopsy was used for two experimental runs per day (morning and afternoon), kept on ice-cold BIOPS for less than 4.5 and 7.7 h, respectively.

2.2. Experimental design

Two experienced scientists prepared the pfi with slightly different preparation procedures they routinely used for mechanical separation of muscle fiber bundles, i.e. sharp forceps or needles. This was the only difference in the standardized pfi preparation (Fig. 1).

Data with a cytochrome *c* control efficiency higher than 0.1 and m_w lower than 0.5 mg were excluded from the final dataset (Fig. S1). The cytochrome *c* control efficiency was calculated in the OXPHOS state following Gnaiger, 2020 [54].

Table 1

Respiration of permeabilized fibers from biopsies of human *vastus lateralis*. Donors differ in age, gender, physical activity, and body mass index BMI. The studies have been conducted using different respiration media, O_2 regimes, presence/absence of contraction inhibitors, and temperature. O_2 flux was normalized for wet or dry tissue mass, m_w or m_d. Abbreviations: Bleb: blebbistatin; BTS: N-benzyltoluene sulfonamide; G: glutamate; M: malate; MiR05: mitochondrial respiration medium MiR05; MiR06: MiR05 plus catalase; *N*: sample size; NA: not available; Oct: octanoylcarnitine; P: pyruvate; Pal: palmitoylcarnitine; Ref: references; Rot: rotenone; S: succinate; *T*: temperature; V_{O2max}: maximum O_2 consumption (cardiorespiratory fitness index); Z: respiration medium Z. Symbols: ♂: males; ♀: females; ~: approximately.

Biometric data	Age	BMI	V_{O2max}	Respi-ration medium	O_2 regime	Coupling and pathway control state	O_2 flux (per m_w) at 37 °C	Ref
	[years]	[kg/m^2]	[mL·min^{-1}·kg^{-1}]		[μM]		[pmol·s^{-1}·mg^{-1}]	
Healthy								
♂ ($N = 8$)	26 ± 2	NA	44 ± 7	MiR05	190–175	GMS_P	~42	[35][c]
♂ ($N = 68$)	31.4 ± 8.2	25.2 ± 3.2	NA	MiR05	450–275	PMS_P	123.1	[36]
♂ ($N = 11$)	20 ± 2	NA	45.1 ± 7.6	MiR05	450–275	PMS_P	~70	[37]
♂ ($N = 10$)	26 ± 2	NA	NA	MiR06	420–250	$OctPGMS_P$	87	[38]
♂ ($N = 16$)	27 ± 3	NA	43 ± 6	MiR06	420–250	$OctPGMS_P$	86.5	[9]
♂ ($N = 10$)	23 ± 1	25 ± 1	46 ± 2	MiR05	200–100	GMS_P	~45	[39]
♂ ($N = 8$)	22 ± 2	NA	45.7 ± 2.1	MiR06	450–280	$PGMS_P$	~72.9[a]	[40]
♂ ($N = 9$)	24 (19–30)	21.4 (19.6–25.7)	54 (49–57)	MiR05	500–200	$PalGMS_P$	55 (47–71)	[41]
♂ ($N = 8$)	26 ± 2	NA	43.8 ± 6.8	MiR05	NA	GMS_P	~27	[42][c]
♂ ($N = 8$)	23 ± 1	23.8 ± 0.6	NA	MiR05 + Bleb	200–180	$PGMS_P$	~142.9[b]	[43]
♀ ($N = 8$)	21 ± 1	24.1 ± 1.6	NA	MiR05 +Bleb	200–180	$PGMS_P$	~142.9[b]	[43]
♂ ($N = 17$)	27 ± 3	NA	47 ± 5	MiR06	420–250	$OctPGMS_P$	103.5	[44]
♂ ($N = 15$)	26.2 ± 5.3	NA	37.9 ± 7.8	MiR05	NA	PM_P	383.4	[45][c]
♂ ($N = 16$)	24.3 ± 0.9	23.4 ± 0.5	50.0 ± 2.4	MiR05	450–200	$PGMS_P$	~70	[20]
♂ ($N = 21$)	26 ± 4	NA	46 ± 5	MiR06	420–250	$OctPGMS_P$	94	[8]
♂ ($N = 5$)	NA	21.6 ± 1.2	NA	Z + BTS	220–150	GM_P	~55.5[a,b]	[47]
♂ ($N = 10$)	27 ± 1	23.5 ± 1.3	40.3 ± 3.0	Z + Bleb	250–	PMS_P	~65	[48]
♂ ($N = 10$) & ♀ ($N = 6$)	31 ± 2	23.6 ± 0.8	48 ± 2	MiR05	400–250	$OctM_P$	~22.5[a]	[21]
♂ ($N = 10$) & ♀ ($N = 6$)	31 ± 2	23.6 ± 0.8	48 ± 2	MiR05	400–250	$OctPGMS_P$	~90[a]	[21]
♂ ($N = 10$)	26 ± 1	24.1	54.43	MiR05	>300	$OctM_P$	~30[a]	[49]
♂ ($N = 10$)	26 ± 1	24.1	54.43	MiR05	>300	$OctGM_P$	~60[a]	[49]
♂ ($N = 10$)	26 ± 1	24.1	54.43	MiR05	>300	$OctGMS_P$	~90[a]	[49]
♂ ($N = 10$)	26 ± 1	24.1	54.43	MiR05	>300	S $(Rot)_P$	~60[a]	[49]
♂ ($N = 7$) & ♀ ($N = 7$)	21 ± 2	NA	49 ± 1	MiR05	400–275	$PalPGM_P$	~35	[50]
♂ ($N = 7$) & ♀ ($N = 7$)	21 ± 2	NA	49 ± 1	MiR05	400–275	PGM_P	~46	[50]
♂ ($N = 7$) & ♀ ($N = 7$)	21 ± 2	NA	49 ± 1	MiR05	400–275	PM_P	~40	[50]
♂ ($N = 7$) & ♀ ($N = 7$)	21 ± 2	NA	49 ± 1	MiR05	400–275	$PalM_P$	~20	[50]
♂ ($N = 7$) & ♀ ($N = 7$)	21 ± 2	NA	49 ± 1	MiR05	400–275	S $(Rot)_P$	~60	[50]
♂ ($N = 8$) & ♀ ($N = 2$)	31.2 ± 5.4	21.3 ± 1.0	56.7 ± 9.6	Z + Bleb	400–200	GMS_P	~90	[19]
♂ ($N = 8$) & ♀ ($N = 2$)	67.5 ± 2.7	24.2 ± 1.0	34.9 ± 4 0.3	Z + Bleb	400–200	GMS_P	~85	[19]
Overweight								
♂ ($N = 18$) & ♀ ($N = 6$)	28 ± 7	26 ± 3	NA	MIR05	400–200	$OctPGMS_P$	46.6	[32]
♂ ($N = 11$) & ♀ ($N = 8$)	70.7 ± 4.7	27.7 ± 0.7	18.6 ± 3.8	Z + Bleb	400–200	GMS_P	~65	[19]
Obese								
♂ ($N = 5$) & ♀ ($N = 7$)	40 ± 2	32 ± 2	27 ± 2	MiR05	450–200	GMS_P	~55	[30]
♂ ($N = 17$) & ♀ ($N = 14$)	62 ± 8	31 ± 6	NA	MiR05	400–200	$OctPGMS_P$	36.1	[32]
♂ ($N = 9$)	57.3 ± 6.5	33 ± 5	21.4 ± 5.4	MiR05	450–300	$OctPMS_P$	~30	[33]
♂ ($N = 20$)	60 ± 2	33.3 ± 0.6	NA	MiR05	450–200	$PGMS_P$	~70	[34]
♂ ($N = 5$)	NA	43.0 ± 4.1	NA	Z + BTS	220–150	GM_P	~37.0[a,b]	[47]
♀ ($N = 24$)	31.6 ± 1.4	30.2 ± 1.4	NA	Z + BTS	220–150	$PalGMS_P$	67.4[a,b]	[31]
♀ ($N = 8$)	35.1 ± 2.4	36.5 ± 2.4	NA	Z + BTS	220–150	$PalGMS_P$	68.4[a,b]	[31]

O_2 fluxes were measured using the Oroboros O2k (Oroboros Instruments, Innsbruck, Austria).
Raw data from Table 1 are shown in Table S1.

[a] Respirometry was performed at 30 °C and O_2 fluxes were adjusted to 37 °C by multiplication with a *T*-factor of 1.62 [22].

[b] Fiber wet mass to dry mass ratio is assumed to be 3.5 [22].

[c] Measured using the Hansatech system (Hansatech Instruments, King's Lynn, United Kingdom).

2.3. Preparation of permeabilized muscle fibers

A portion of the muscle sample was mechanically permeabilized immediately after biopsy collection (morning) while the other half was kept on ice-cold BIOPS and was prepared in the afternoon. After removal of visible blood and connective tissue, fiber bundles were gently teased apart by two experienced researchers using two different procedures: (*1*) needles (BD microlance; 23G, BD, NJ, USA) under a magnifying glass or (*2*) a pair of sharp forceps (Fisher Scientific, Item#50822410) under a dissecting microscope (Zeiss, Stemi 305, Jena, Germany) using a small Petri dish (ThermoFisher Scientific, Item#150318) and an ice block (Biocision, Item#BCS-132). Muscle samples were kept completely submerged in ice-cold BIOPS during both procedures. Immediately after mechanical separation, fiber bundles (form by 15–25 fibers or several with less fibers) were incubated in 5 mL of ice-cold BIOPS containing freshly prepared saponin (50 μg saponin/mL BIOPS). After 30 min shaking on ice for chemical permeabilization of the plasma membrane, fiber bundles were washed by continuous shaking for 10 min in either 5 mL ice-cold MiR05 or medium Z. Finally, pfi were blotted on blotting paper for 5 s, transferred to another dry section of the blotting paper for 2 s, and the m_w was measured (range 0.60–2.83 mg) on a calibrated microbalance (Mettler Toledo, XS105, Columbus, USA) as previously described [28].

In our study, we did not find significant differences related to the two mechanical fiber bundle separations in pfi preparation (Fig. S3). It is important to mention that in this study both operators had extensive experience preparing permeabilized human muscle fibers.

2.4. High-resolution respirometry

O_2 consumption of human pfi was measured at 37 °C by high-resolution respirometry (HRR) with the Oxygraph-2k (O2k; Oroboros Instruments, Innsbruck, Austria) in pre-calibrated 2 mL chambers with continuous stirring (750 rpm) [28]. Four experimental conditions were compared using two mitochondrial respiration media, MiR05 (Oroboros MiR05-Kit Lot#0915) and medium Z (prepared according to Table S2) in two different O_2 regimes, low O_2 (L: 200-100 μM) and high O_2 (H: 400-250 μM): (*1*) MiR05 in the absence of Bleb and presence of the vehicle DMSO (MiR05-Bleb), (*2*) MiR05 with 25 μM Bleb (MiR05+Bleb), (*3*) medium Z in the absence of Bleb and presence of the vehicle DMSO (*Z*-Bleb), and (*4*) medium Z in the presence of 25 μM Bleb (Z+Bleb). Due to the photosensitivity of Bleb [55], illumination of the O2k chambers was switched off after addition of Bleb/DMSO. The increase of the O_2 concentration in experiments performed at the high O_2 regime was achieved by the injection of O_2 gas into the gas phase of the open O2k chambers. The researchers preparing pfi and operators running the experiments were blind to each chamber experimental condition (except for the oxygen regime).

We applied the substrate–uncoupler–inhibitor titration protocol SUIT-008 (Fig. 2) [56]. First, NADH- (N-) linked substrates (5 mM pyruvate, 2 mM malate; PM) were titrated immediately after the addition of permeabilized fibers and Bleb/DMSO. Subsequently, the O_2 concentration was increased in experiments conducted at high O_2 levels. LEAK respiration (PM_L) was determined after the addition of pyruvate and malate for low O_2, or after the O_2 concentration was increased for high O_2, once O_2 fluxes stabilized. Then, a kinetically saturating concentration of ADP (5 mM) with $MgCl_2{\cdot}6H_2O$ (3 mM) was added to evaluate N-pathway OXPHOS capacity (PM_P). After testing the integrity of the mitochondrial outer membrane by adding cytochrome *c* (10 μM), glutamate (10 mM) was added as additional N-linked substrate (PGM_P). Succinate (10 mM) was injected to assess OXPHOS-capacity of the convergent N- and succinate-pathway into Q (NS-pathway, $PGMS_P$). Additional ADP titrations were performed to ensure kinetically saturating concentrations for OXPHOS capacity [57]. The uncoupler carbonyl cyanide-*p*-trifluoromethoxyphenylhydrazone (FCCP) was titrated stepwise to obtain ET-capacity of the NS-pathway ($PGMS_E$). Since ET-capacity must be at least equal ($E = P$) or higher ($E > P$) than OXPHOS capacity, $E < P$ is due to an experimental artefact (e.g. application of an inhibitory uncoupler concentration) [54]. If $PGMS_E$ showed slightly lower values compared to $PGMS_P$, $PGMS_E$ was corrected as $PGMS_E = PGMS_P$. Afterwards, Complex I was inhibited by rotenone (0.5 μM), allowing the evaluation of the succinate- (S-) pathway ET-capacity (S_E). Finally, Complex III was inhibited by antimycin A (2.5 μM) to measure residual O_2 consumption (*Rox* in the ROX state). O_2 concentrations were maintained within low and high O_2 ranges by opening-closing the experimental chamber or by adding O_2 into the gas phase of the open O2k chambers. O_2 fluxes were corrected for the respective instrumental O_2 background. For real-time data acquisition and analysis, DatLab 7.4 software (Oroboros Instruments, Innsbruck, Austria) was employed. Marks to obtain data of the O_2 fluxes were

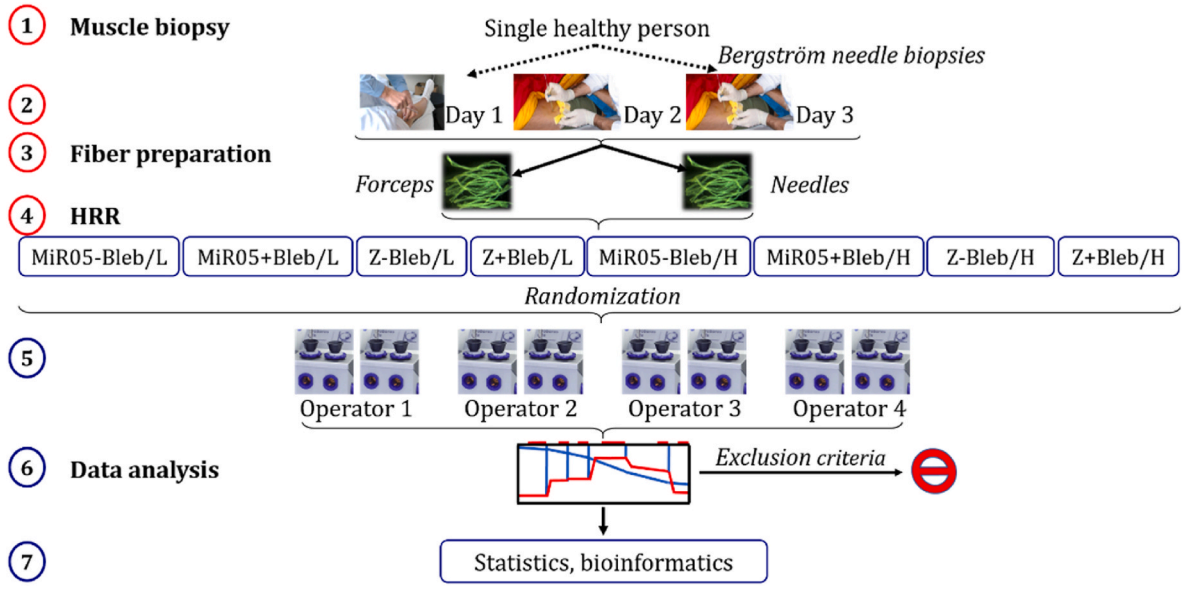

Fig. 1. Workflow of the human *vastus lateralis* study. Abbreviations: HRR: high-resolution respirometry; MiR05: mitochondrial respiration medium MiR05; Z: respiration medium Z; ± Bleb: presence/absence of blebbistatin; L: low O_2 regime (200-100 μM); H: high O_2 regime (400-250 μM). Each operator used two O2k with all-together 16 experimental chambers each morning and afternoon on three consecutive days.

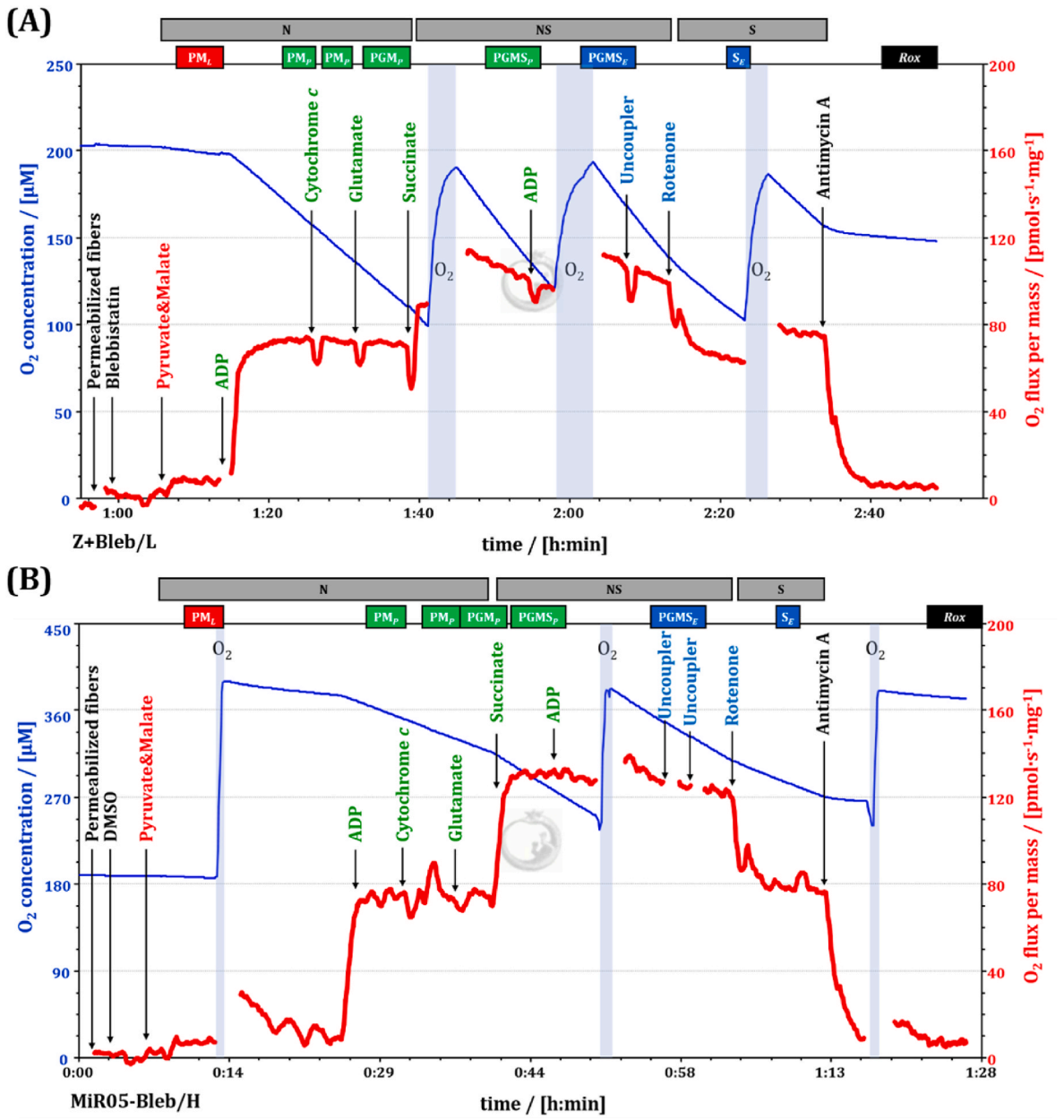

Fig. 2. Representative traces of respiration of pfi from human *vastus lateralis*. High-resolution respirometry with two O_2 regimes and two respiration media with the substrate-uncoupler-inhibitor titration protocol SUIT-008. Blue lines: O_2 concentration [µM], red lines: mass-specific O_2 flux [pmol•s^{-1}•mg^{-1}] as a function of time. **(A)** Low O_2 (L, 200-100 µM), medium Z with blebbistatin (+Bleb); **(B)** high O_2 (H, 400-250 µM), MiR05, absence of blebbistatin (-Bleb). Additions: permeabilized fibers, 25 µM blebbistatin or vehicle (DMSO); 5 mM pyruvate and 2 mM malate supporting the NADH-pathway N in the LEAK state (PM_L); ADP: kinetically saturating ADP concentration to measure OXPHOS capacity (PM_P); 10 µM cytochrome *c* to evaluate the mitochondrial outer membrane integrity; 10 mM glutamate as additional N-linked substrate (PGM_P); 10 mM succinate to activate the convergent electron flow into Q in the NADH&succinate-pathway NS ($PGMS_P$); ADP: further ADP addition to assess saturating ADP concentrations; U: uncoupler titrations to obtain the electron transfer-capacity ($PGMS_E$); 0.5 µM rotenone to inhibit Complex I (S_E); 2.5 µM antimycin A (Complex III inhibitor) to measure residual O_2 consumption (*Rox*, ROX state). Shaded areas indicate addition of O_2 gas into the gas phase while the chamber was opened for reoxygenation. The chamber illumination was switched off during respirometric measurements. Artefacts in the O_2 flux (spikes) due to reoxygenations and chemical additions were eliminated from the traces.

performed when a steady state was reached at each step of the SUIT protocol, indicating stable O_2 flux over time (red line, in Fig. 2).

2.5. *Microscopic analysis of mitochondria network integrity and ultrastructure*

A fraction of the skeletal muscle biopsy was fixed freshly, and subfractions of the biopsy were fixed after defined preparatory and experimental steps: after dissection and permeabilization, and in samples obtained from the O2k-chambers after completion of respirometric measurements. Fixation was performed by immersion in 2 % glutaraldehyde, or 2 % paraformaldehyde supplemented with 0.15 % picric acid, for electron microscopy and light microscopy, respectively. For electron microscopy, muscle fibers were post-fixed with 1 % osmium in 0.1 M Sorensen buffer (pH 7.4) for 20 min. Muscle fibers were then dehydrated in a graded series of ethanol, transferred to propylene oxide, and embedded in Epon according to standard procedures. Ultrathin sections were cut with a Reichert-Jung Ultracut E microtome and collected on one-hole copper grids with Formvar supporting membranes. Sections were stained with uranyl acetate and lead citrate and

examined with a CM 100 transmission electron microscope (FEI, Termofisher, Waltham, USA) operated at an accelerating voltage of 80 kV. Images were collected using a Megaview 2 camera and processed with the Analysis software package.

For fluorescence confocal microscopy analysis, single muscle fibers were isolated and mitochondrial networks were labelled by immunostaining with a rabbit anti-COX IV (1:500, Ab16056, Abcam) primary antibody, immunodetected with a goat anti-rabbit conjugated to Alexa 488 (1:500, Thermofisher, Waltham, USA). Image acquisition was performed with a LSM700 (Carl Zeiss, Jena, Germany), through a Plan-Apochromat 63x/1.4 objective. Confocal z-stacks from the surface of the fiber and 10 μm in following Nyquist criterion (Voxel size x, y, z – 90,•90,•280 nm).

2.6. Statistics

To identify the systematic differences in measurements of O_2 fluxes that lead to predictable outcomes of the procedure, we followed two complementary approaches: (*1*) a leave-one-out (LOO) cross-validation strategy using a Random Forest Classifier to predict unobserved features; (*2*) a LOO cross-validation using a Random Forest regressor to predict each individual O_2 flux. For each O_2 flux at different respiratory states we computed Spearman's correlation between predicted and observed O_2 flux values.

Statistical analysis was performed using the software GraphPad Prism 9. Non-parametric Mann-Whitney test was applied. Data are shown as median ± interquartile range.

3. Results

3.1. Mitochondrial network and ultrastructure

Human pfi preparations were assessed by electron and confocal microscopy to evaluate how the permeabilization procedure and

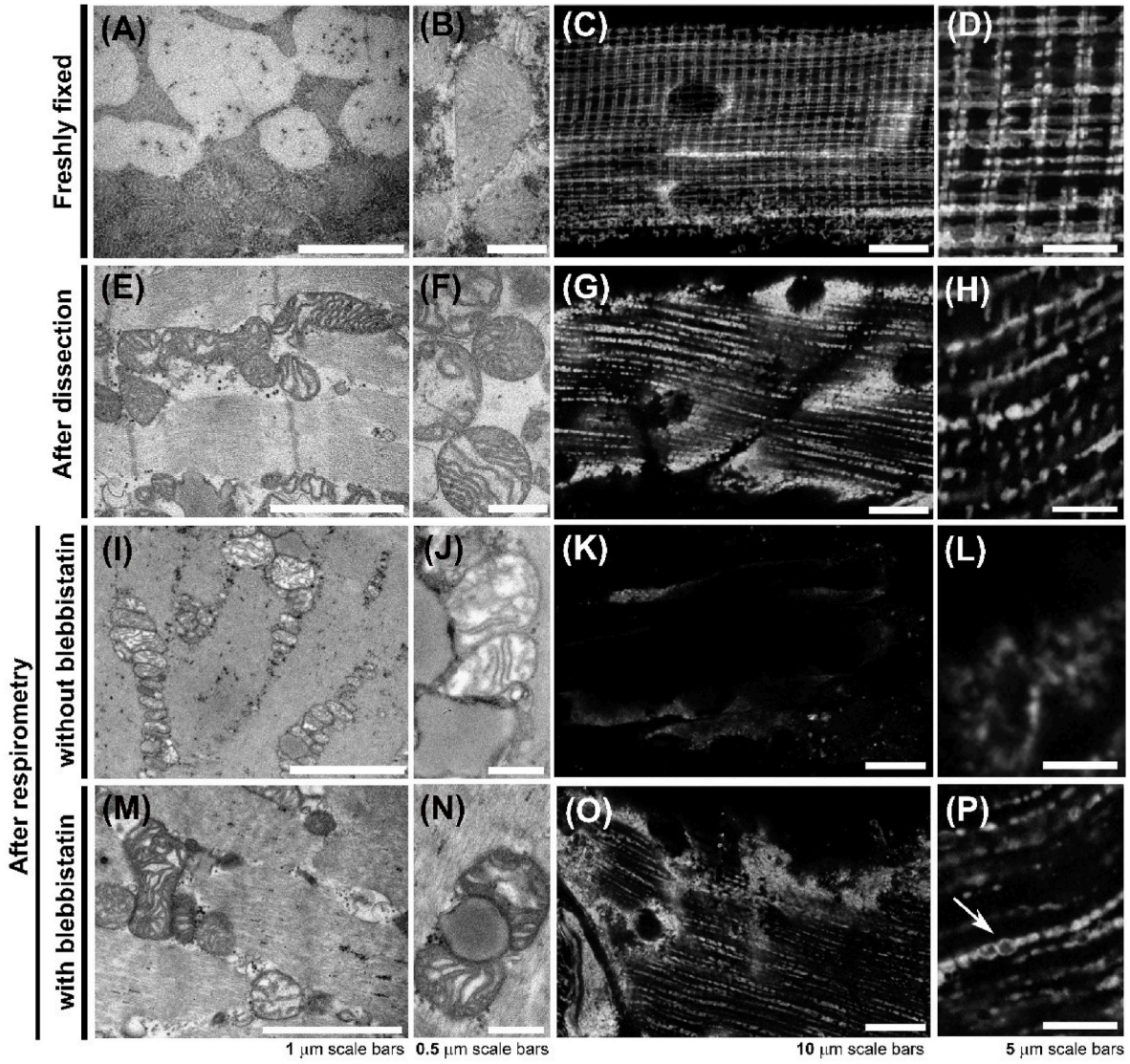

Fig. 3. Effect of sample preparation and incubation on the mitochondrial network and ultrastructure. Sample fractions were fixed for light and electron microscopy. **(A–D)** Mitochondria from freshly fixed muscle fibers were highly connected and displayed dense and preserved cristae**. (E–H)** Dissection and permeabilization with saponin induced mitochondrial fragmentation and disruption of ultrastructural integrity, including swelling, and bursting of mitochondria. **(H)** Mitochondrial fragmentation occurred in both longitudinal and transversal connections. **(I–P)** After completion of titration protocol SUIT-008 in the respirometric chambers, muscle fibers were fixed and analyzed with electron and confocal microscopy. Respirometric incubation induced further fragmentation and swelling of mitochondria, **(I–L)** especially in absence of blebbistatin. **(M, N)** Mitochondrial ultrastructure was better preserved in fibers incubated with blebbistatin, compared to **(I, J)** fibers incubated in absence of blebbistatin. Scale bars are indicated under each panel column.

mitochondrial respirometry incubations affect mitochondrial ultrastructure and network integrity compared to muscle fibers fixed before these procedures (Fig. 3A–D). Although these analyzes were conducted on a limited number of samples, these images show that the dissection and permeabilization of muscle fibers bundles induce mitochondrial fragmentation (Fig. 3E–H). Transversal connections between intermyofibrillar mitochondria decreased and different degrees of longitudinal fragmentation were observed. These effects of dissection and permeabilization were independent on respiration media (MiR05 versus medium Z) used. The structural preservation of mitochondrial networks and ultrastructure of the cristae were highly compromised in the fibers after respirometric measurements (Fig. 3I–P). Addition of Bleb to the incubation medium seems to improve the preservation of the mitochondrial morphology. Fibers incubated without Bleb showed enlarged mitochondria, with disrupted inner and outer membranes (Fig. 3J). The isolated fibers that were incubated with Bleb showed better preservation of the mitochondrial membrane ultrastructure, although several largely swollen mitochondria were detected per fiber as well (Fig. 3P, arrow). Thus, respirometric measurements in pfi are performed in fragmented mitochondria regardless of the original organization of the skeletal muscle mitochondrial networks *in vivo*.

Despite our results indicating that the presence of Bleb in the

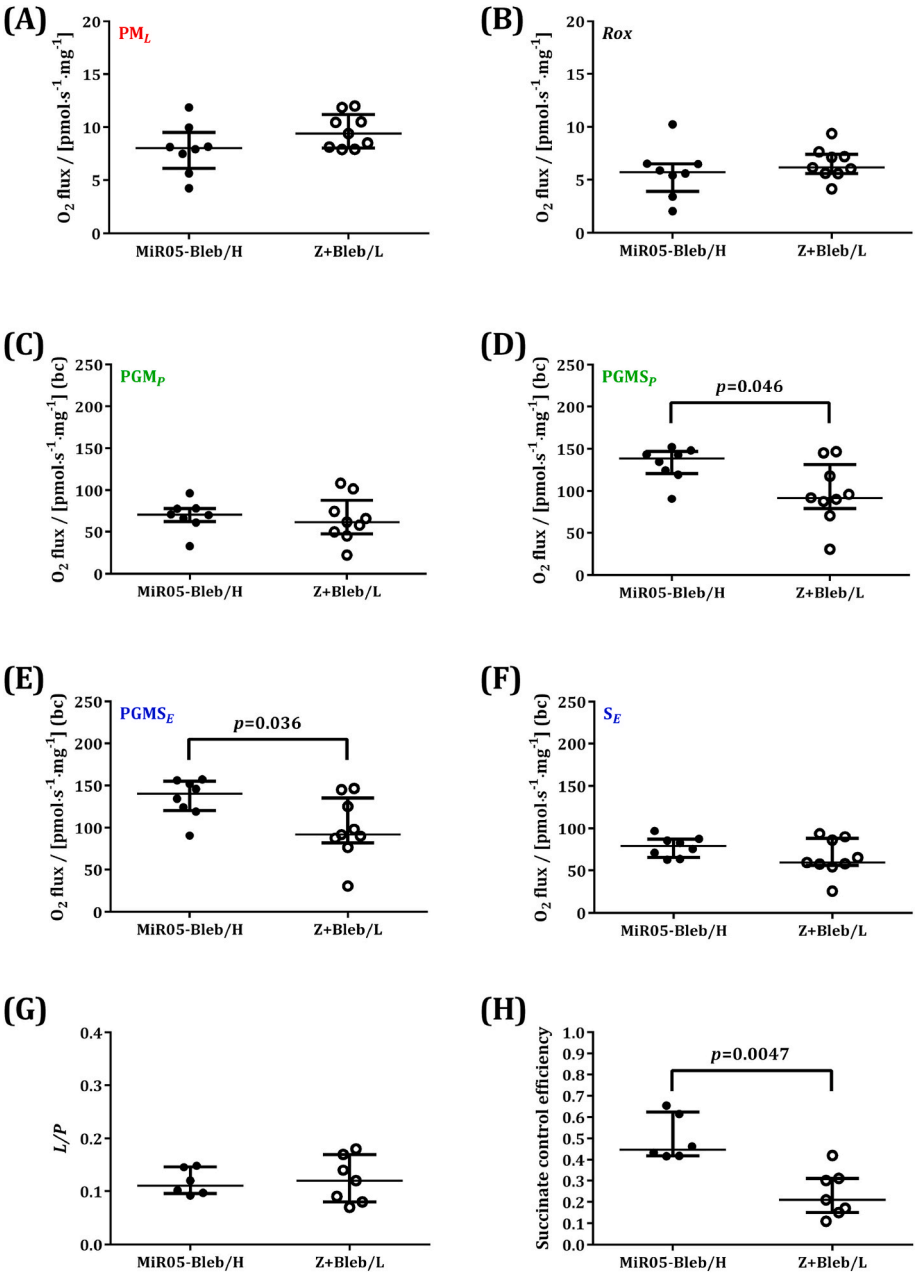

Fig. 4. Comparison of experimental respirometric conditions in permeabilized human skeletal muscle fibers. Respiration in MiR05 at high O_2 without blebbistatin (MiR05-Bleb/H) compared to medium Z at low O_2 with blebbistatin (Z + Bleb/L). **(A)** Mass-specific O_2 fluxes [pmol•s^{-1}•mg^{-1}] corrected (bc) and non-corrected for residual O_2 consumption (*Rox*) in LEAK state supported by pyruvate and malate (PM_L); **(B)** Residual oxygen consumption *Rox* after inhibiting Complex III with antimycin A. **(C, D)** OXPHOS capacity in the presence of pyruvate, glutamate and malate (PGM_P) or NS-linked pathway after addition of succinate ($PGMS_P$). **(E, F)** ET capacity of the NS- ($PGMS_E$) or S-pathway after inhibition of Complex I by rotenone (S_E). **(G)** Coupling-control ratio (L/P) calculated as PM_L/PM_P, and **(H)** succinate control efficiency calculated as $1\text{-}J_{O2}(PGM_P)/J_{O2}(PGMS_P)$. Results are represented as scatter plots and median with interquartile range from individual human muscle fiber preparations (n = 7–9) obtained from three biopsies (N = 3) of the same volunteer. p-values from Mann-Whitney tests. Total respiration not corrected for *Rox* is shown in Fig. S2.

respiration medium seems to preserve the mitochondrial membrane ultrastructure (Fig. 3), it is important to mention that the use of Bleb did not influence mitochondrial respiration (Fig. S4) or cytochrome *c* control efficiency (Fig. S1). This indicates that the presence or absence of Bleb in the respiration medium does not affect the release of cytochrome *c* induced by sample preparation in human permeabilized muscle fibers. Therefore, Bleb should not be used as a strategy to decrease cytochrome *c* control efficiency.

3.2. Comparison of experimental conditions to study mitochondrial respiration in pfi

As shown in Table 1, different experimental conditions (i.e. respiration medium, use of contraction inhibitors, O_2 regime) are used in studies evaluating mitochondrial respiration in human pfi. Studies performed in MiR05 are commonly carried out at a high O_2 regime in the absence of Bleb, whereas studies in medium Z are conventionally done at low O_2 regime in the presence of Bleb [19,36,37,48]. Consequently, we compared mitochondrial respiratory capacity (Fig. 2) of pfi in MiR05 and high O_2 regime (400-250 μM O_2) and medium Z with Bleb and low O_2 regime (200-100 μM O_2; Fig. 4). Differences were not apparent between both experimental conditions in N-linked pathway states, both in the LEAK (PM_L) and OXPHOS (PGM_P) states (Fig. 4A and C). Similarly, mass specific ET-capacity in the S-pathway (S_E) did not show significant differences between experimental conditions (Fig. 4F). However, when O_2 flux was further increased from the N-pathway by addition of succinate to induce convergent electron transfer into the Q-junction (Fig. 4D and E), a significant difference was observed in OXPHOS: $PGMS_P$, MiR05-Bleb/H: 139 pmol•s^{-1}•mg^{-1} (121−147 pmol•s^{-1}•mg^{-1}); Z + Bleb/L: 92 pmol•s^{-1}•mg^{-1} (79−131 pmol•s^{-1}•mg^{-1}) $p = 0.046$, and ET states: $PGMS_E$, MiR05-Bleb/H: 140 pmol•s^{-1}•mg^{-1} (121−155 pmol•s^{-1}•mg^{-1}); Z + Bleb/L: 92 pmol•s^{-1}•mg^{-1} (82−135 pmol•s^{-1}•mg^{-1}) $p = 0.036$ between the two experimental regimes.

In addition, we evaluated two qualitative parameters of mitochondrial function. No differences were found for the coupling-control ratio at low N-linked pathway flux (*L/P*; Fig. 4G) but a significant reduction was observed for the stimulatory effect of succinate (succinate control efficiency) addition to N-linked substrates (MiR05-Bleb/H: 0.45 (0.42−0.62); Z + Bleb/L: 0.21 (0.15−0.31), $p = 0.0047$; Fig. 4H).

In conclusion, the variability among previously published studies (Table 1) cannot be attributed only to physiological characteristics of the study groups, but lab-to-lab variability and differences in standard operating procedures must be considered. Under controlled experimental conditions (Fig. 1), experimental variables impact on the apparent mitochondrial performance. These variables include composition of respiration media, the use of Bleb, and O_2 regime as previously suggested [22].

3.3. Predictive analysis of potential factors contributing to experimental variability

To identify the systematic differences in measurements of O_2 fluxes that lead to predictable outcomes of the procedure, we followed two complementary approaches. The first approach assessed whether it is possible to predict a particular feature (factor; i.e. experimental day, experimental run, pfi preparation, respiration medium, O_2 regime, presence/absence Bleb, O2k-operator and experimental O2k-chamber) using the O_2 flux obtained in a specific experimental assay. Specifically, we followed a leave-one-out (LOO) cross-validation strategy using a Random Forest Classifier (RFC) to predict unobserved features. That is, to predict the feature of a certain experimental condition (target feature such as respiration medium), we trained the RFC model with all results on O_2 flux in all assays and their corresponding features leaving out only the assay (O_2 flux and target feature) for which we wanted to predict the target feature. We repeated this process for all assays and obtained an average prediction accuracy as the fraction of correctly predicted target features. To assess whether the average accuracy was higher than expected (which would indicate a correlation between feature and O_2 flux), we randomized target features. That is, we matched target features to O_2 flux vectors at random, and we repeated the same LOO strategy as for real data. We repeated the randomization process 1000 times to obtain a distribution of randomly expected average prediction accuracies. By comparing the actual prediction accuracy of the target feature to the random expectation, we assigned a *p*-value to the measured accuracy. We found that two features were significantly correlated with O_2 flux: O_2 regime and respiration medium (Table 2, Fig. 5A and B). The confusion matrices from LOO experiments for these two features clearly show that most of the time it is possible to predict the correct O_2 regime and respiration medium 23/32 for low O_2 and 29/35 for high O_2; 23/31 for medium Z and 24/33 for MiR05 (Fig. 5A and B). Remarkably, when we performed the LOO prediction experiments for the combination of the two features (O_2 regime and respiration medium), it is possible to correctly predict respiration media for high O_2 regimes but not for low O_2 regimes (12/19 for high O_2 regime and medium Z; and 12/16 for high O_2 regime and MiR05; Fig. 5C). These results point to a clear difference in high O_2 flux readouts for high O_2 regimes (400-250 μM), in relation to the respiration medium used.

Our second approach included all features used previously to predict each specific O_2 flux measurement (O_2 flux for PM_L, PGM_P, $PGMS_P$, $PGMS_E$ and S_E; Fig. 6). Again, we followed a LOO cross-validation using a RFC to predict each individual O_2 flux. For each O_2 flux at different respiratory states we computed Spearman's correlation between predicted and observed O_2 flux. To assess whether these correlations were different from random, we repeated the process by randomizing the features 1000 times and obtained the distribution of randomly expected Spearman's rho values. Fig. 6 shows that by using all features, we can predict PM_L, $PGMS_P$, $PGMS_E$ and S_E but not PM_P and PGM_P. Additionally, by using only O_2 regime and respiration media (green line, Fig. 6) the correlation between predicted and real fluxes was close to the correlation obtained for predictions with all features (except for PM_L, where some other feature seems to play a role, S_E was marginally significant).

Both complementary statistical analyses revealed significant differences, clearly indicating that results on O_2 flux depend on the tested experimental regimes, specifically on the respiration medium and O_2 regime. This predictive analysis of potential factors contributing to experimental variability strongly shows that the other potential

Table 2
Statistics of leave-one-out prediction experiments (LOO). Random forest classifier (RFC) to predict unobserved data in leave-one-out experiments for each one of the features considered using O_2 readouts as training (see results section). LOORF Accuracy is the average accuracy of the RFC for that feature. Av. Accuracy Random is the average accuracy obtained for LOO when the features were randomized (1000 times). *p*-values computed by comparing the LOORF to the distribution of accuracies obtained from the randomizations of each feature. Abbreviations: pfi: permeabilized fibers; MiR05: mitochondrial respiration medium MiR05; Z: medium Z; L: low O_2 regime; H: high O_2 regime; Bleb (±): presence/absence of blebbistatin.

Column	*p*-value	LOO RF	Av. Accuracy	Significance 0.05/9
Day (1,2,3)	0.5773	0.3125	0.3199	n.s
Run (1: morning, 2: afternoon)	0.7469	0.4688	0.5110	n.s.
pfi prep (needle/forceps)	0.0561	0.6563	0.5258	n.s.
Respiration medium (MiR05/Z)	0.0027	0.7031	0.4856	significant
O_2 regime (L/H)	0.0014	0.7969	0.4956	significant
Bleb (+/-)	0.2524	0.5469	0.4855	n.s.
O2k-operator	0.0096	0.4375	0.2620	n.s.
O2k-chamber	0.6077	0.0469	0.0507	n.s.
O_2 regime/respiration medium	0.0014	0.5625	0.2367	significant

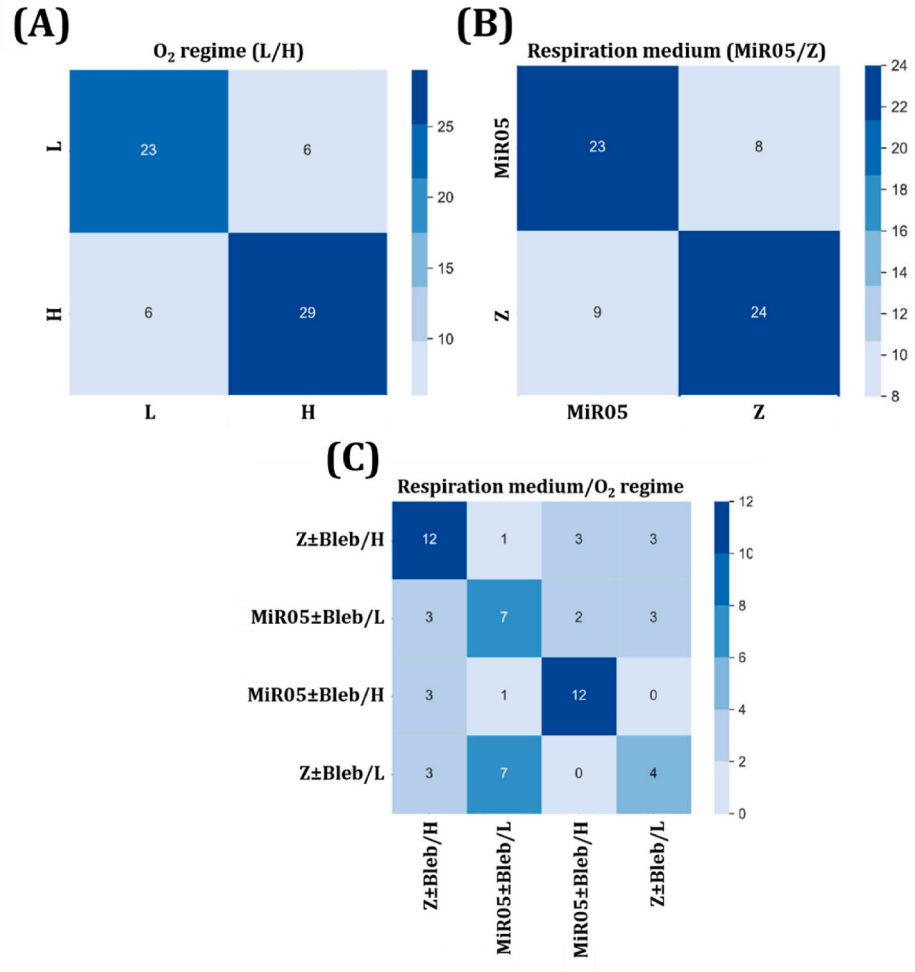

Fig. 5. Confusion matrix for predictions of O_2 regime and respiration medium. Results for leave-one-out prediction experiments using a Random Forest Classifier (RFC) for the following features: **(A)** O_2 regime, **(B)** respiration medium, **(C)** combination of both. Rows indicate predicted feature classes, while columns indicate real (true) feature classes. Elements along the diagonal correspond to accurately classified data, while off-diagonal matrix elements correspond to misclassified data. Matrix elements are colored according to the color bars on the right-hand side of each matrix: the darker the color, the larger the RFC. The RFC identified O_2 regime and respiration medium from O_2 flux readouts. However, the analysis of the combination of O_2 regime and respiration medium shows that differences in respiration media were only detectable for high O_2 regimes. Abbreviations: L: low O_2 regime; H: high O_2 regime; MiR05: mitochondrial respiration medium MiR05; Z: medium Z; ±Bleb combination of data in the presence and absence of blebbistatin.

variables (two standardized pfi preparations, time of the day, consecutive day of the experiment) did not influence our results, nor did the standardized variables (O2k-operator, O2k-chamber) exert any influence on the results.

3.4. *Targeted statistical analysis of critical features in high-resolution respirometry*

To validate results obtained by the leave-on-out (LOO) cross-validation method using Random Forest models, more specific statistical analyses were performed to assess the influence of each parameter of interest in HRR experiments under the current experimental conditions.

Effect of the myosin inhibitor blebbistatin: To assess the influence of Bleb in human pfi preparation on O_2 flux, we compared its use with both respiratory media (MiR05 and medium Z) under both O_2 regimes (low O_2 at 200-100 μM and high O_2 at 400-250 μM). The addition of Bleb in the O2k chamber did not exert any effect on mitochondrial respiration (Fig. 7).

These results corroborate previous predictions by leave-on-out (LOO) cross-validation method using Random Forest models where the use of the myosin inhibitor Bleb, independently or in combination with other features, was unable to predict O_2 fluxes when saturating substrate concentrations are used.

O_2 regime: One of the features that predicted the observed differences in O_2 fluxes was the O_2 regime used in human pfi respiratory studies. In this regard, the O_2 dependence of mitochondrial respiration in pfi has been previously reported, about 100-fold higher p_{50} compared to small living cells and isolated mitochondria [58,59]. One of the arguments published in favour of using Bleb is the option of avoiding high O_2 regimes to assess mitochondrial respiration [60] by inhibiting *in vitro* skeletal muscle fiber contraction and by this means to reduce the O_2 dependence. However, the prevention of O_2 dependence under low O_2 regimes using Bleb was not adequately addressed in this study [60]. Our results clearly show that Bleb does not exert any impact on mitochondrial respiration regardless of the O_2 regime used (Fig. S4).

Due to the absence of any Bleb effect on mitochondrial respiration, we combined data with and without Bleb to assess the effects of respiration media in both O_2 regimes (Fig. 8).

Our results confirm that O_2 concentration in the experimental O2k-chamber influences mitochondrial respiration of pfi in MiR05 (Fig. 8A). When medium Z is used (with or without Bleb) such sensitivity to O_2 concentration is absent (Fig. 8B). However, when comparing OXPHOS capacities in the NS-pathway ($PGMS_P$) measured in both respiratory media at high O_2 regime, respiration was lower in medium Z (Fig. 8B).

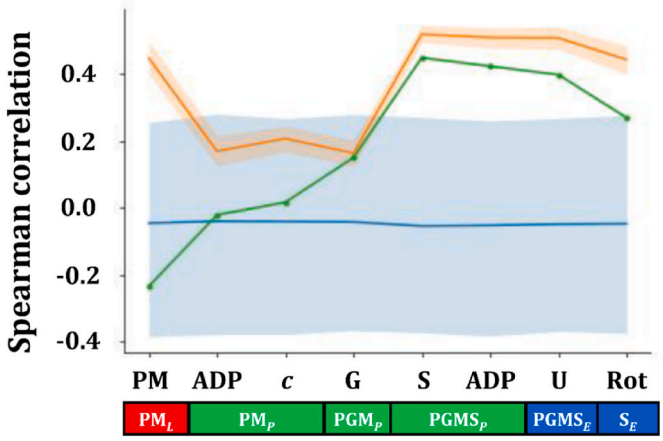

Fig. 6. Predictability of individual O_2 fluxes. LOO cross-validation experiments using a Random Forest regressor to predict individual O_2 flux (*x*-axis). Prediction accuracy was quantified by Spearman's correlation (*y*-axis) between predicted and measured flux. The orange line shows the correlation values obtained from the RFC model using all available features (experimental day, experimental run, pfi preparation, respiration medium, O_2 regime, presence/absence of blebbistatin, O2k-operator, and O2k-chamber) as predictors. The green line shows Spearman's correlation values using respiration medium and O_2 regime as predictors of O_2 flux. The blue line and shaded region are the 95 % C.I. for the random expectation, obtained when all feature values are randomized. Points in orange that fall out of the shaded region show O_2 flux that can be predicted from the features. Abbreviations: P: pyruvate; M: malate; *c*: cytochrome *c*; G: glutamate; S: succinate; U: uncoupler; Rot: rotenone; *L*: LEAK respiration; *P*: OXPHOS capacity; *E*: ET capacity.

3.5. Correction factors for respiration medium and O_2 concentration

To elucidate if differences of mitochondrial respiration in $PGMS_P$ between MiR05 and medium Z (Fig. 8) depend on the O2k-operator performance or O_2 regime conditions, we applied correction factors to the O_2 fluxes (Fig. 9 and Fig. S5).

First, an O_2 correction factor was calculated for each respiration medium as the median values of the O_2 fluxes at high-O_2 divided by median values of O_2 fluxes at low-O_2. Since the presence of Bleb in the O2k chamber has not any effect on mitochondrial respiration (Fig. 7 and Fig. S4), combined data with and without Bleb were used to calculate the correction factors. These correction factors were 1.56 and 1.24 for MiR05 and medium Z, respectively. O_2 fluxes at low-O_2 were multiplied with O_2 correction factors for each respiration medium.

Second, O_2 fluxes obtained in experiments performed with respiration medium Z were multiplied by the media correction factor 1.33 (media correction factor of medium Z: median values of O_2 fluxes in MiR05/median values of O_2 fluxes in medium Z). The application of O_2- and media-correction factors showed that the differences between both media are not related to the O2k performance between operators (Fig. S5). Consequently, O_2 fluxes at respiratory state $PGMS_P$ in MiR05 and medium Z were multiplied with O_2 correction factors. Results indicate that there are differences related to the respiration media used, which are independent of O_2 regimes (Fig. 9).

4. Discussion

This study evaluated current preanalytical and analytical procedures for high-resolution respirometry, routinely used to assess mitochondrial function in human pfi. Several international groups with specific experience in the field convened at the same laboratory to collaborate and perform the present study. The intention was to minimize technical sources of variability and therefore reinforce the study's ability to infer insight into the effect of experimental regimes on respiration of permeabilized human muscle fibers.

Previous research has explored how varying fitness levels and body compositions correspond to a range of 60–180 pmol O_2 s^{-1} mg^{-1} in skeletal muscle maximal OXPHOS capacity, with the lower end typical of sedentary individuals with obesity and the upper end representative of athletes [22]. Exercise factors, such as training volume and intensity, can influence various mitochondrial parameters, including protein synthesis, content, and respiratory function—both mass-specific and mitochondrial-specific respiration. Granata et al. (2018) provided evidence that training volume significantly affects mitochondrial content, whereas exercise intensity primarily drives changes in mass-specific mitochondrial respiration [61]. Their comprehensive analysis highlighted the dissociation between mitochondrial content and respiratory function, revealing how different training strategies can uniquely influence skeletal muscle mitochondrial adaptations. A precise knowledge of these factors is critical to optimize training programs and athletes' performance.

Based on current literature it is difficult to derive solid conclusions on the "optimal experimental procedure" or to combine published datasets for in-depth meta-analysis. Mainly due to differences in the selected experimental conditions – respiration media and O_2 regime – as potential major sources of variability among studies (Table 1).

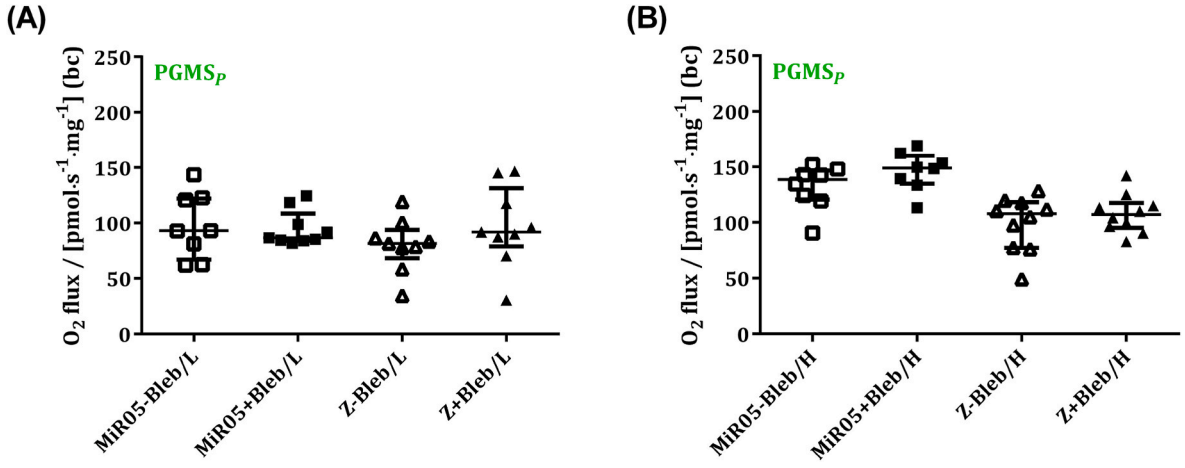

Fig. 7. No effect of blebbistatin on mitochondrial respiration. Evaluation of Bleb effect on OXPHOS capacity supporting NS-pathway ($PGMS_P$) at **(A)** low and **(B)** high O_2 regimes in respiration media MiR05 and Z. Results are represented as scatter plots and median with interquartile range from individual human muscle fiber preparations ($n = 8$–10) obtained from three biopsies ($N = 3$) of the same volunteer. Abbreviations: MiR05: mitochondrial respiration medium MiR05; Z: medium Z; ± Bleb: presence/absence of blebbistatin; L: low O_2; H: high O_2; bc: baseline correction by residual O_2 consumption.

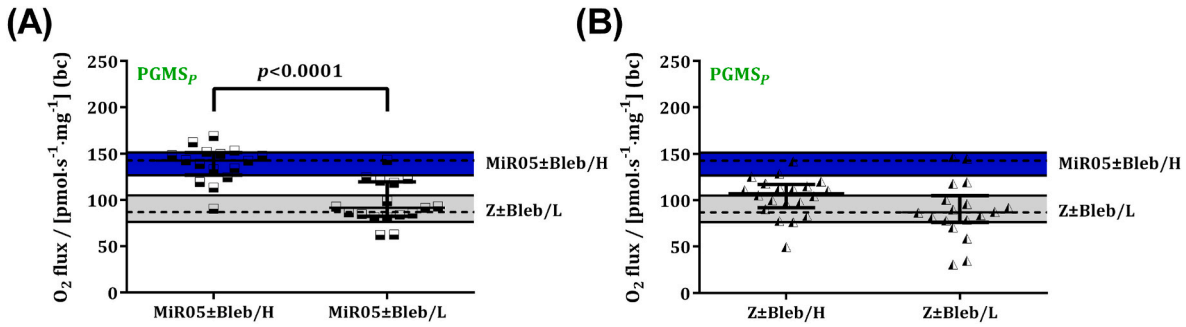

Fig. 8. O_2 regime influences mitochondrial respiration in permeabilized human skeletal fibers. NS-pathway OXPHOS respiratory capacity ($PGMS_P$) at low and high O_2 regimes using **(A)** respiration medium MiR05 and **(B)** medium Z. Dashed and solid lines show the median and interquartile ranges, respectively, obtained in MiR05 in the presence&absence of Bleb at high O_2 regime (MiR05±Bleb/H, blue) and in medium Z in the presence&absence of Bleb at low O_2 (Z ± Bleb/L, gray). Results are represented as scatter plots and medians with interquartile range from individual human muscle fiber preparations (n = 16–20) obtained from three biopsies (N = 3) of the same volunteer. p-values indicate the level of significance obtained from Mann-Whitney tests. Abbreviations: MiR05: mitochondrial respiration medium MiR05; Z: medium Z; ±Bleb: combination of data in the presence and absence of blebbistatin; L: low O_2 regime; H: high O_2 regime; bc: baseline correction by residual O_2 consumption.

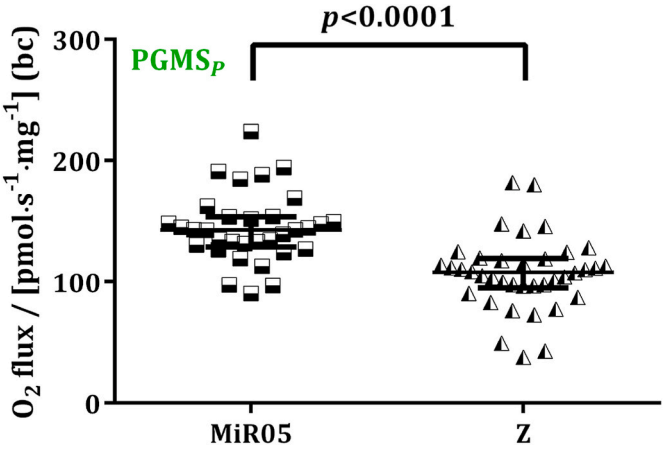

Fig. 9. Effect of respiration medium on O_2 flux ($PGMS_P$) after application of correction factors for the O_2 regime. Results are represented as scatter plots and medians with interquartile ranges from individual human muscle fiber preparations (n = 33–38) obtained from three biopsies (N = 3) of the same volunteer. p-values from Mann-Whitney tests. Correction factors: O_2 (MiR05) = 1.56, O_2(Z) = 1.24. Abbreviations: NS_P: NS-pathway OXPHOS capacity; MiR05: mitochondrial respiration medium MiR05; Z: medium Z; bc: baseline correction by residual O_2 consumption.

However, there is a growing need for standardization of experimental conditions to generate comparable results among studies. This is a necessary step to build reliable opensource datasets that facilitate Bayesian statistics and obtain answers to relevant questions raised by scientists studying human muscle mitochondrial function as a diagnostic readout to assess athletes' performance. By minimizing sources of variability and standardization of technical variables, this study identified two critical experimental conditions with a significant effect on O_2 flux of permeabilized human muscle fibers: respiration medium and O_2 regime.

Environmental O_2 levels, O_2 delivery and respiratory metabolism are the main factors controlling cellular oxygenation. Physiological intracellular O_2 concentrations are significantly lower than ambient O_2 levels at normoxic conditions. Thus, when working with cells or isolated mitochondria, air saturation will mimic a hyperoxic environment when assessing mitochondrial performance [62,63]. Therefore, when HRR studies are performed using living or permeabilized cells, or isolated mitochondria, O_2 concentration in the experimental chamber could be below 1 kPa, due to the low p_{50} and O_2 diffusion distance; this O_2 concentration in the chamber is at least 10 times higher than the p_{50}, which ranges from 0.01 to 0.10 kPa in mitochondria and small cells [58,59]. However, an O_2 dependence was already reported [57] when high-resolution respirometry studies were performed in skeletal muscle pfi due to a higher diffusion distance (from 5 to 10 μm in cells to >150 μm in the intertwined fiber bundles [58] increasing significantly p_{50} values in more than 50 orders of magnitude, from below 0.1 kPa in small cells to 5 kPa in permeabilized muscle fiber bundles).

The effect of respirometric incubation on disruption of the mitochondrial network caused by preparation and respirometric incubation on respiratory capacities may be limited, considering that the measurements are performed in pfi, where substrates reach mitochondria by entering through the membrane pores made by the permeabilization step and directly diffuse across the cytoplasm, instead of reaching specific mitochondria and travelling through mitochondrial networks [64].

Our current results agree with previous observations in rat muscle but disagree with previous findings in human *vastus lateralis* muscle. Unfortunately, that specific study did not report data in human muscle at air saturating and higher O_2 regimes, making a comparison with our study results difficult [60].

When comparing MiR05 and medium Z, our results show that differences in mitochondrial respiration of permeabilized human fibers in NS_P ($PGMS_P$) remain after applying O_2 and operator correction factors (Fig. 9). We investigate the respiration media composition (Table S2) to identify other potential factors which may trigger the observed difference in mitochondrial respiration between medium Z and MiR05. It has been described that chloride inhibits OXPHOS and ET capacities using different substrate combinations [65]. In this study, Wollenman et al. addressed that chloride may inhibit adenine nucleotide translocase and substrate transport across the inner mitochondrial membrane [65]. Moreover, another study showed an inhibitory effect of chloride on the mitochondrial creatine kinase [66]. The presence of higher concentration of chloride in medium Z (46 mM after addition of ADP + $MgCl_2$) compared to the respiration medium MiR05 (12 mM after addition of ADP + $MgCl_2$) may explain the lower NS_P which we observed in medium Z. Other components present in MiR05 i.e. taurine and K-lactobionate may play a role protecting mitochondrial function.

Current efforts to optimize and standardize the biological relevance of HRR studies [36,54,67,68] are of major interest for different stakeholders: scientific research, athletic performance, clinical practice, and companies working on research and development in fields related to mitochondrial function assessment. The European COST-action MitoEAGLE had as an objective to improve our knowledge on mitochondrial function in health and disease related to Evolution, Age, Gender, Lifestyle and Environment (EAGLE). For such undertaken, a well-coordinated international network worked on the harmonization of protocols towards generating a rigorously monitored data repository on

mitochondrial respiratory function. An initial and necessary step was to ameliorate dissemination and inter-study data analysis by standardization and harmonization of terminology [54] which is a critical step for data recording, building up inter-laboratory databases and comparison of datasets. The incapacity to harmonize previous published data sets using HRR in muscle tissues takes the working group 2 of the European COST-action MitoEAGLE to concentrate on the optimization of HRR studies in muscle tissues as a major task that has been divided in two main actions: (*1*) inter-laboratory study on human permeabilized myofibers: effects of fiber preparation, respiration medium and Bleb on mitochondrial respiratory capacity and O_2 regime; (*2*) inter-laboratory harmonization of protocols for mitochondrial function evaluation in muscle pfi. The current manuscript is a result of these actions. Thus, the results presented in this study move forward the goal of achieving reliable HRR measurements, which together with the valuable information supplied by other methodological studies [36,54,67,68] brings closer the idea of establishing unified experimental conditions and defining a HRR protocol that allows inter-study comparisons, which it is of great need and demand nowadays. However, Cardinale et al. clearly pointed out other potential sources of variability (e.g. sample preparation) that should be taken into consideration when studies are performed by different researchers with different technical skills [67]. Research in methodological harmonization and optimization will benefit consortia, such as the Molecular Transducers of Physical Activity Consortium (MoTrPAC). MoTrPAC aims to generate a molecular map of exercise by using a multi-omic approach and bioinformatic analysis, both in preclinical and clinical studies [69]. Ancillary projects from MoTrPAC and SOMMA are focused on mitochondrial function assessment in human skeletal muscle and will be a significant contribution to the Consortium.

5. Conclusions

Our results demonstrate that O_2 fluxes in human skeletal muscle pfi are significantly influenced by the media and O_2 regime. Thus, we conclude that high O_2 regime (400-250 μM) and a buffer composition that do not interfere with the measurements, such as in this case MiR05, are the optimal conditions to assess mitochondrial respirometry in human skeletal muscle pfi. Our study provides a basis to harmonize results on human skeletal muscle pfi and establishes guidelines for selecting optimum experimental conditions, contributing to fight the reproducibility crisis. These experimental advances will facilitate a more accurate assessment of athletic performance and human health.

Data availability statement

Original files are available Open Access at Zenodo repository: https://doi.org/10.5281/zenodo.7229481.

Ethics approval statement

The study was approved by the local ethics committee of Copenhagen and Frederiksberg in Denmark (hs:h-15002266). All procedures were carried out in accordance with the declaration of Helsinki.

CRediT authorship contribution statement

Carolina Doerrier: Writing – review & editing, Writing – original draft, Visualization, Validation, Methodology, Investigation, Formal analysis, Data curation, Conceptualization, Supervision. **Pau Gama-Perez:** Methodology, Investigation, Formal analysis, Data curation. **Dominik Pesta:** Writing – review & editing, Methodology, Investigation, Formal analysis, Data curation, Conceptualization. **Giovanna Distefano:** Writing – review & editing, Methodology, Investigation. **Stine D. Soendergaard:** Methodology, Investigation. **Karoline Maise Chroeis:** Investigation, Methodology. **Alba Gonzalez-Franquesa:** Methodology, Investigation. **Bret H. Goodpaster:** Validation, Resources, Conceptualization. **Clara Prats:** Writing – review & editing, Methodology, Investigation, Formal analysis. **Marta Sales-Pardo:** Writing – review & editing, Writing – original draft, Visualization, Validation, Methodology, Formal analysis, Data curation. **Roger Guimera:** Writing – review & editing, Writing – original draft, Visualization, Validation, Methodology, Formal analysis, Data curation. **Paul M. Coen:** Writing – review & editing, Writing – original draft, Validation, Data curation. **Erich Gnaiger:** Writing – review & editing, Visualization, Validation, Software, Resources, Funding acquisition, Data curation, Conceptualization. **Steen Larsen:** Writing – review & editing, Writing – original draft, Visualization, Validation, Supervision, Resources, Methodology, Funding acquisition, Formal analysis, Data curation, Conceptualization. **Pablo M. Garcia-Roves:** Writing – review & editing, Writing – original draft, Visualization, Validation, Supervision, Project administration, Methodology, Investigation, Funding acquisition, Formal analysis, Data curation, Conceptualization.

Declaration of competing interest

The authors declare no competing interests.

Acknowledgements

CD has been employed by Oroboros Instruments. GD is a recipient of the Postdoctoral Fellowship Award from the American Diabetes Association (1-19-PDF-006). This publication is based upon work from COST Action CA15203 MitoEAGLE, supported by COST (European Cooperation in Science and Technology; https://wiki.oroboros.at/index.php/COST_Action_MitoEAGLE).

Appendix A. Supplementary data

Supplementary data to this article can be found online at https://doi.org/10.1016/j.freeradbiomed.2024.07.039.

Abbreviations

Ama	antimycin A	N	NADH-linked pathway
Bleb	blebbistatin	NA	not available
BTS	N-benzyl-P-toluenesulfonamide	NS	NADH- and succinate-linked pathway
c	cytochrome *c*	O_2	oxygen
CI	Complex I	Oct	octanoylcarnitine
CIII	Complex III	OXPHOS	oxidative phosphorilation
D	ADP	*P*	capacity of oxidative phosphorylation, OXPHOS capacity
E	electron transfer capacity, ET capacity	P	pyruvate
FCCP	carbonyl cyanide *p*-trifluoro-methoxyphenyl hydrazone	Pal	palmitoylcarnitine
G	glutamate	pfi	permeabilized fibers

(*continued on next page*)

(*continued*)

H	high oxygen regime	RF	Random Forest
HRR	high-resolution respirometry	Rot	rotenone
J_{O2}	mass-specific O_2 flux	*Rox*	residual oxygen consumption; ROX: state of *Rox*
L	LEAK respiration	S	succinate
L	Low oxygen regime	SUIT	substrate-uncoupler-inhibitor titration
LOO	leave-one-out cross-validation	U	uncoupler
M	malate	Z	mitochondrial respiration medium Z, medium Z
m_d	dry mass		
MiR05	mitochondrial respiration medium 5		
m_w	wet mass		

References

[1] E. Gnaiger, et al., MitoEAGLE Task Group, Mitochondrial physiology, Bioenergetics Communications 2020 (2020) 1, https://doi.org/10.26124/bec:2020-0001.v1.

[2] M. Wiese, A.J. Bannister, Two genomes, one cell: mitochondrial-nuclear coordination via epigenetic pathways, Mol. Metabol. 38 (2020) 100942, https://doi.org/10.1016/j.molmet.2020.01.006.

[3] P. Lisowski, P. Kannan, B. Mlody, A. Prigione, Mitochondria and the dynamic control of stem cell homeostasis, EMBO Rep. 19 (5) (2018) e45432, https://doi.org/10.15252/embr.201745432.

[4] M.R. Duchen, G. Szabadkai, Roles of mitochondria in human disease, Essays Biochem. 47 (2010) 115–137, https://doi.org/10.1042/bse0470115.

[5] B. Egan, A.P. Sharples, Molecular responses to acute exercise and their relevance for adaptations in skeletal muscle to exercise training, Physiol. Rev. 103 (3) (2023) 2057–2170, https://doi.org/10.1152/physrev.00054.2021.

[6] R. Furrer, J.A. Hawley, C. Handschin, The molecular athlete: exercise physiology from mechanisms to medals, Physiol. Rev. 103 (3) (2023) 1693–1787, https://doi.org/10.1152/physrev.00017.2022.

[7] J.P. Little, A. Safdar, G.P. Wilkin, M.A. Tarnopolsky, M.J. Gibala, A practical model of low-volume high-intensity interval training induces mitochondrial biogenesis in human skeletal muscle: potential mechanisms, J. Physiol. 588 (2010) 1011–1022, https://doi.org/10.1113/jphysiol.2009.181743.

[8] A.K. Meinild Lundby, R.A. Jacobs, S. Gehrig, J. de Leur, M. Hauser, T.C. Bonne, D. Flück, S. Dandanell, N. Kirk, A. Kaech, U. Ziegler, S. Larsen, C. Lundby, Exercise training increases skeletal muscle mitochondrial volume density by enlargement of existing mitochondria and not de novo biogenesis, Acta Physiol. 222 (1) (2018) e12905, https://doi.org/10.1111/apha.12905.

[9] R.A. Jacobs, D. Flück, T.C. Bonne, S. Bürgi, P.M. Christensen, M. Toigo, C. Lundby, Improvements in exercise performance with high-intensity interval training coincide with an increase in skeletal muscle mitochondrial content and function, J. Appl. Physiol. 115 (6) (2013) 785–793, https://doi.org/10.1152/japplphysiol.00445.2013.

[10] D. Pesta, F. Hoppel, C. Macek, H. Messner, M. Faulhaber, C. Kobel, W. Parson, M. Burtscher, M. Schocke, E. Gnaiger, Similar qualitative and quantitative changes of mitochondrial respiration following strength and endurance training in normoxia and hypoxia in sedentary humans, Am. J. Physiol. Regul. Integr. Comp. Physiol. 301 (4) (2011), https://doi.org/10.1152/ajpregu.00285.2011.

[11] C.F. McKenna, A.F. Salvador, A.R. Keeble, N.A. Khan, M. De Lisio, A.R. Konopka, S. A. Paluska, N.A. Burd, Muscle strength after resistance training correlates to mediators of muscle mass and mitochondrial respiration in middle-aged adults, J. Appl. Physiol. 133 (3) (2022) 572–584, https://doi.org/10.1152/japplphysiol.00186.2022.

[12] M. Flockhart, L.C. Nilsson, S. Tais, B. Ekblom, W. Apro, F.J. Larsen, Excessive exercise training causes mitochondrial functional impairment and decreases glucose tolerance in healthy volunteers, Cell Metabol. 33 (2021) 957–970 e6, https://doi.org/10.1016/j.cmet.2021.02.017.

[13] J.A. Hawley, D.J. Bishop, High-intensity exercise training - too much of a good thing? Nat. Rev. Endocrinol. 17 (7) (2021) 385–386, https://doi.org/10.1038/s41574-021-00500-6.

[14] C. López-Otín, M.A. Blasco, L. Partridge, M. Serrano, G. Kroemer, The hallmarks of aging, Cell 153 (6) (2013) 1194–1217, https://doi.org/10.1016/j.cell.2013.05.039.

[15] L. Galluzzi, E. Morselli, O. Kepp, I. Vitale, A. Rigoni, E. Vacchelli, M. Michaud, H. Zischka, M. Castedo, G. Kroemer, Mitochondrial gateways to cancer, Mol. Aspect. Med. 31 (1) (2010) 1–20, https://doi.org/10.1016/j.mam.2009.08.002.

[16] M. Bonora, M.R. Wieckowski, D.A. Sinclair, G. Kroemer, P. Pinton, L. Galluzzi, Targeting mitochondria for cardiovascular disorders: therapeutic potential and obstacles, Nat. Rev. Cardiol. 16 (1) (2019) 33–55, https://doi.org/10.1038/s41569-018-0074-0.

[17] B.B. Lowell, G.I. Shulman, Mitochondrial dysfunction and type 2 diabetes, Science 307 (5708) (2005) 384–387, https://doi.org/10.1126/science.1104343.

[18] R.A. Standley, G. Distefano, M.B. Trevino, E. Chen, N.R. Narain, B. Greenwood, G. Kondakci, V.v. Tolstikov, M.A. Kiebish, G. Yu, F. Qi, D.P. Kelly, R.B. Vega, P. M. Coen, B.H. Goodpaster, J. Magaziner, Skeletal muscle energetics and mitochondrial function are impaired following 10 days of bed rest in older adults, J. Gerontol.: Series A 75 (9) (2020) 1744–1753, https://doi.org/10.1093/gerona/glaa001.

[19] G. Distefano, R.A. Standley, X. Zhang, E.A. Carnero, F. Yi, H.H. Cornnell, P. M. Coen, Physical activity unveils the relationship between mitochondrial energetics, muscle quality, and physical function in older adults, Journal of Cachexia, Sarcopenia and Muscle 9 (2) (2018) 279–294, https://doi.org/10.1002/jcsm.12272.

[20] S. Larsen, M. Hey-Mogensen, R. Rabøl, N. Stride, J.W. Helge, F. Dela, The influence of age and aerobic fitness: effects on mitochondrial respiration in skeletal muscle, Acta Physiol. 205 (3) (2012) 423–432, https://doi.org/10.1111/j.1748-1716.2012.02408.x.

[21] E. Gnaiger, R. Boushel, H. Søndergaard, T. Munch-Andersen, R. Damsgaard, C. Hagen, C. Díez-Sánchez, I. Ara, C. Wright-Paradis, P. Schrauwen, M. Hesselink, J.A.L. Calbet, M. Christiansen, J.W. Helge, B. Saltin, Mitochondrial coupling and capacity of oxidative phosphorylation in skeletal muscle of Inuit and Caucasians in the arctic winter, Scand. J. Med. Sci. Sports 25 (2015) 126–134, https://doi.org/10.1111/sms.12612.

[22] E. Gnaiger, Capacity of oxidative phosphorylation in human skeletal muscle. New perspectives of mitochondrial physiology, Int. J. Biochem. Cell Biol. 41 (10) (2009) 1837–1845, https://doi.org/10.1016/j.biocel.2009.03.013.

[23] P.M. Coen, E.v. Menshikova, G. Distefano, D. Zheng, C.J. Tanner, R.A. Standley, N. L. Helbling, G.S. Dubis, V.B. Ritov, H. Xie, M.E. Desimone, S.R. Smith, M. Stefanovic-Racic, F.G.S. Toledo, J.A. Houmard, B.H. Goodpaster, Exercise and weight loss improve muscle mitochondrial respiration, lipid partitioning, and insulin sensitivity after gastric bypass surgery, Diabetes 64 (11) (2015) 3737–3750, https://doi.org/10.2337/db15-0809.

[24] L.M. Sparks, L.M. Redman, K.E. Conley, M.E. Harper, F. Yi, A. Hodges, A. Eroshkin, S.R. Costford, M.E. Gabriel, C. Shook, H.H. Cornnell, E. Ravussin, S.R. Smith, Effects of 12 Months of caloric restriction on muscle mitochondrial function in healthy individuals, J. Clin. Endocrinol. Metabol. 102 (1) (2017) 111–121, https://doi.org/10.1210/jc.2016-3211.

[25] S. Larsen, R. Rabøl, C.N. Hansen, S. Madsbad, J.W. Helge, F. Dela, Metformin-treated patients with type 2 diabetes have normal mitochondrial complex i respiration, Diabetologia 55 (2) (2012) 443–449, https://doi.org/10.1007/s00125-011-2340-0.

[26] M.J. Torres, K.A. Kew, T.E. Ryan, E.R. Pennington, C. te Lin, K.A. Buddo, A.M. Fix, C.A. Smith, L.A. Gilliam, S. Karvinen, D.A. Lowe, E.E. Spangenburg, T.N. Zeczycki, S.R. Shaikh, P.D. Neufer, 17β-estradiol directly lowers mitochondrial membrane microviscosity and improves bioenergetic function in skeletal muscle, Cell Metabol. 27 (1) (2018) 167–179, https://doi.org/10.1016/j.cmet.2017.10.003, e7.

[27] M. Picard, T. Taivassalo, G. Gouspillou, R.T. Hepple, Mitochondria: isolation, structure and function, J. Physiol. 589 (18) (2011) 4413–4421, https://doi.org/10.1113/jphysiol.2011.212712.

[28] C. Doerrier, L.F. Garcia-Souza, G. Krumschnabel, Y. Wohlfarter, A.T. Mészáros, E. Gnaiger, High-Resolution FluoRespirometry and OXPHOS protocols for human cells, permeabilized fibers from small biopsies of muscle, and isolated mitochondria, Methods Mol. Biol. 1782 (2018) 31–70, https://doi.org/10.1007/978-1-4939-7831-1_3.

[29] L. Scandalis, D.W. Kitzman, B.J. Nicklas, M. Lyles, P. Brubaker, M.B. Nelson, M. Gordon, J. Stone, J. Bergstrom, P.D. Neufer, E. Gnaiger, A.J.A. Molina, Skeletal muscle mitochondrial respiration and exercise intolerance in patients with heart failure with preserved ejection fraction, JAMA Cardiolology (2023) e230957, https://doi.org/10.1001/jamacardio.2023.0957. Epub ahead of print.

[30] T.L. Dohlmann, M. Hindsø, F. Dela, J.W. Helge, S. Larsen, High-intensity interval training changes mitochondrial respiratory capacity differently in adipose tissue and skeletal muscle, Physiological Reports 6 (18) (2018) e13857, https://doi.org/10.14814/phy2.13857.

[31] D.A. Kane, C. te Lin, E.J. Anderson, H.B. Kwak, J.H. Cox, P.M. Brophy, R. C. Hickner, P. Darrell Neufer, R.N. Cortright, Progesterone increases skeletal muscle mitochondrial H2O2 emission in nonmenopausal women, Am. J. Physiol. Endocrinol. Metab. 300 (3) (2011) 528–535, https://doi.org/10.1152/ajpendo.00389.2010.

[32] C. Porter, N.M. Hurren, M.v. Cotter, N. Bhattarai, P.T. Reidy, E.L. Dillon, W. J. Durham, D. Tuvdendorj, M. Sheffield-Moore, E. Volpi, L.S. Sidossis, B. B. Rasmussen, E. Børsheim, Mitochondrial respiratory capacity and coupling control decline with age in human skeletal muscle, Am. J. Physiol. Endocrinol. Metab. 309 (3) (2015) E224–E232, https://doi.org/10.1152/ajpendo.00125.2015.

[33] A.J. Trewin, I. Levinger, L. Parker, C.S. Shaw, F.R. Serpiello, M.J. Anderson, G. K. McConell, D.L. Hare, N.K. Stepto, Acute exercise alters skeletal muscle mitochondrial respiration and H2O2 emission in response to hyperinsulinemic-

euglycemic clamp in middle-aged obese men, PLoS One 12 (11) (2017) e0188421, https://doi.org/10.1371/journal.pone.0188421.
[34] O.L. Dollerup, S. Chubanava, M. Agerholm, S.D. Søndergård, A. Altıntaş, A. B. Møller, K.F. Høyer, S. Ringgaard, H. Stødkilde-Jørgensen, G.G. Lavery, R. Barrès, S. Larsen, C. Prats, N. Jessen, J.T. Treebak, Nicotinamide riboside does not alter mitochondrial respiration, content or morphology in skeletal muscle from obese and insulin-resistant men, J. Physiol. 598 (4) (2020) 731–754, https://doi.org/10.1113/jp278752.
[35] M.T. Lewis, G.M. Blain, C.R. Hart, G. Layec, M.J. Rossman, S.Y. Park, J.D. Trinity, J.R. Gifford, S.K. Sidhu, J.C. Weavil, T.J. Hureau, J.E. Jessop, A.D. Bledsoe, M. Amann, R.S. Richardson, Acute high-intensity exercise and skeletal muscle mitochondrial respiratory function: role of metabolic perturbation, Am. J. Physiol. Regul. Integr. Comp. Physiol. 321 (5) (2021) R687–R698, https://doi.org/10.1152/ajpregu.00158.2021.
[36] M. Jacques, J. Kuang, D.J. Bishop, X. Yan, J. Alvarez-Romero, F. Munson, A. Garnham, I. Papadimitriou, S. Voisin, N. Eynon, Mitochondrial respiration variability and simulations in human skeletal muscle: the Gene SMART study, FASEB (Fed. Am. Soc. Exp. Biol.) J. : Official Publication of the Federation of American Societies for Experimental Biology 34 (2) (2020) 2978–2986, https://doi.org/10.1096/fj.201901997rr.
[37] C. Granata, R.S.F. Oliveira, J.P. Little, K. Renner, D.J. Bishop, Mitochondrial adaptations to high-volume exercise training are rapidly reversed after a reduction in training volume in human skeletal muscle, Faseb. J. 30 (10) (2016) 3413–3423, https://doi.org/10.1096/fj.201500100r.
[38] P.M. Christensen, R.A. Jacobs, T. Bonne, D. Flöck, J. Bangsbo, C. Lundby, A short period of high-intensity interval training improves skeletal muscle mitochondrial function and pulmonary oxygen uptake kinetics, J. Appl. Physiol. 120 (11) (2016) 1319–1327, https://doi.org/10.1152/japplphysiol.00115.2015.
[39] M.J. MacInnis, E. Zacharewicz, B.J. Martin, M.E. Haikalis, L.E. Skelly, M. A. Tarnopolsky, R.M. Murphy, M.J. Gibala, Superior mitochondrial adaptations in human skeletal muscle after interval compared to continuous single-leg cycling matched for total work, J. Physiol. 595 (9) (2017) 2955–2968, https://doi.org/10.1113/jp272570.
[40] G. Vincent, S. Lamon, N. Gant, P.J. Vincent, J.R. MacDonald, J.F. Markworth, J. A. Edge, A.J.R. Hickey, Changes in mitochondrial function and mitochondria associated protein expression in response to 2-weeks of high intensity interval training, Front. Physiol. 6 (FEB) (2015) 51, https://doi.org/10.3389/fphys.2015.00051.
[41] M. Brands, J. Hoeks, H.P. Sauerwein, M.T. Ackermans, M. Ouwens, N.M. Lammers, M.N. van der Plas, P. Schrauwen, A.K. Groen, M.J. Serlie, Short-term increase of plasma free fatty acids does not interfere with intrinsic mitochondrial function in healthy young men, Metab. Clin. Exp. 60 (10) (2011) 1398–1405, https://doi.org/10.1016/j.metabol.2011.02.006.
[42] G. Layec, G.M. Blain, M.J. Rossman, S.Y. Park, C.R. Hart, J.D. Trinity, J.R. Gifford, S.K. Sidhu, J.C. Weavil, T.J. Hureau, M. Amann, R.S. Richardson, Acute high-intensity exercise impairs skeletal muscle respiratory capacity, Med. Sci. Sports Exerc. 50 (12) (2018) 2409–2417, https://doi.org/10.1249/mss.0000000000001735.
[43] P.M. Miotto, C. McGlory, T.M. Holloway, S.M. Phillips, G.P. Holloway, Sex differences in mitochondrial respiratory function in human skeletal muscle, Am. J. Physiol. Regul. Integr. Comp. Physiol. 314 (6) (2018) R909–R915, https://doi.org/10.1152/ajpregu.00025.2018.
[44] P. Robach, T. Bonne, D. Flück, S. Bürgi, M. Toigo, R.A. Jacobs, C. Lundby, Hypoxic training: effect on mitochondrial function and aerobic performance in hypoxia, Med. Sci. Sports Exerc. 46 (10) (2014) 1936–1945, https://doi.org/10.1249/mss.0000000000000321.
[45] T. Ghiarone, V.A. Andrade-Souza, S.K. Learsi, F. Tomazini, T. Ataide-Silva, A. Sansonio, M.P. Fernandes, K.L. Saraiva, R.C.B.Q. Figueiredo, Y. Tourneur, J. Kuang, A.E. Lima-Silva, D.J. Bishop, Twice-a-day training improves mitochondrial efficiency, but not mitochondrial biogenesis, compared with once-daily training, J. Appl. Physiol. 127 (3) (2019) 713–725, https://doi.org/10.1152/japplphysiol.00060.2019.
[46] A.R. Konopka, W.M. Castor, C.A. Wolff, R.v. Musci, J.J. Reid, J.L. Laurin, Z. J. Valenti, K.L. Hamilton, B.F. Miller, Skeletal muscle mitochondrial protein synthesis and respiration in response to the energetic stress of an ultra-endurance race, J. Appl. Physiol. 123 (6) (2017) 1516–1524, https://doi.org/10.1152/japplphysiol.00457.2017.
[47] E.J. Anderson, M.E. Lustig, K.E. Boyle, T.L. Woodlief, D.A. Kane, C. te Lin, J. W. Price, L. Kang, P.S. Rabinovitch, H.H. Szeto, J.A. Houmard, R.N. Cortright, D. H. Wasserman, P.D. Neufer, Mitochondrial H2O2 emission and cellular redox state link excess fat intake to insulin resistance in both rodents and humans, J. Clin. Invest. 119 (3) (2009) 573–581, https://doi.org/10.1172/JCI37048.
[48] M.L. Dirks, P.M. Miotto, G.H. Goossens, J.M. Senden, H.L. Petrick, J. van Kranenburg, L.J.C. van Loon, G.P. Holloway, Short-term bed rest-induced insulin resistance cannot be explained by increased mitochondrial H2O2 emission, J. Physiol. 598 (1) (2020) 123–137, https://doi.org/10.1113/jp278920.
[49] R.A. Jacobs, R. Boushel, C. Wright-Paradis, J.A.L. Calbet, P. Robach, E. Gnaiger, C. Lundby, Mitochondrial function in human skeletal muscle following high-altitude exposure, Exp. Physiol. 98 (1) (2012) 245–255, https://doi.org/10.1113/expphysiol.2012.066092.
[50] A.J. Chicco, C.H. Le, E. Gnaiger, H.C. Drever, J.B. Muyskens, A. D'Alessandro, T. Nemkov, A.D. Hocker, J.E. Prenni, L.M. Wolfe, N.M. Sindt, A.T. Lovering, A. W. Subudhi, R.C. Roach, Adaptive remodeling of skeletal muscle energy metabolism in high-altitude hypoxia: lessons from AltitudeOmics, J. Biol. Chem. 293 (18) (2018) 6659–6671, https://doi.org/10.1074/jbc.RA117.000470.
[51] J. Bergstrom, Percutaneous needle biopsy of skeletal muscle in physiological and clinical research, Scand. J. Clin. Lab. Investig. 35 (1975) 609–616, https://doi.org/10.1080/00365517509095787.
[52] V.I. Veksler, A.V. Kuznetsov, V.G. Sharov, V.I. Kapelko, A. Saks, Mitochondrial respiratory parameters in cardiac tissue: a novel method of assessment by using saponin-skinned fibres, Biochim. Biophys. Acta, Bioenerg. 892 (1987) 191–196, https://doi.org/10.1016/0005-2728(87)90174-5.
[53] T. Letellier, M. Malgat, M. Coquet, B. Moretto, F. Parrot-Roulaud, J.-P. Mazat, Mitochondrial myopathy studies on permeabilized muscle fibres, Pediatr. Res. 32 (1992) 17–22, https://doi.org/10.1203/00006450-199207000-00004.
[54] E. Gnaiger, Mitochondrial pathways and respiratory control, Bioenergetics Communications (2020) 2, https://doi.org/10.26124/bec:2020-0002, 2020.
[55] B.H. Várkuti, M. Képiró, I.A. Horváth, L. Végner, S. Ráti, A. Zsigmond, G. Hegyi, Z. Lenkei, M. Varga, A. Málnási-Csizmadia, A highly soluble, non-phototoxic, non-fluorescent blebbistatin derivative, Sci. Rep. 6 (2016) 26141, https://doi.org/10.1038/srep26141.
[56] H. Lemieux, P.U. Blier, E. Gnaiger, Remodeling pathway control of mitochondrial respiratory capacity by temperature in mouse heart: electron flow through the Q-junction in permeabilized fibers, Sci. Rep. 7 (2017) 2840, https://doi.org/10.1038/s41598-017-02789-8.
[57] D. Pesta, E. Gnaiger, High-Resolution respirometry: OXPHOS protocols for human cells and permeabilized fibers from small biopsies of human muscle, Methods Mol. Biol. 810 (2012) 25–58, https://doi.org/10.1007/978-1-61779-382-0_3.
[58] E. Gnaiger, Oxygen conformance of cellular respiration: a perspective of mitochondrial physiology, Adv. Exp. Med. Biol. 543 (2003) 39–55, https://doi.org/10.1007/978-1-4419-8997-0_4.
[59] F.M. Scandurra, E. Gnaiger, Cell respiration under hypoxia: facts and artefacts in mitochondrial oxygen kinetics, Adv. Exp. Med. Biol. 662 (2010) 7–25, https://doi.org/10.1007/978-1-4419-1241-1_2.
[60] C.G.R. Perry, D.A. Kane, C. te Lin, R. Kozy, B.L. Cathey, D.S. Lark, C.L. Kane, P. M. Brophy, T.P. Gavin, E.J. Anderson, P.D. Neufer, Inhibiting myosin-ATPase reveals a dynamic range of mitochondrial respiratory control in skeletal muscle, Biochem. J. 437 (2) (2011) 215–222, https://doi.org/10.1042/bj20110366.
[61] C. Granata, N.A. Jamnick, D.J. Bishop, Training-induced changes in mitochondrial content and respiratory function in human skeletal muscle, Sports Med. 48 (8) (2018) 1809–1828, https://doi.org/10.1007/s40279-018-0936-y.
[62] E. Gnaiger, G. Méndez, S.C. Hand, High phosphorylation efficiency and depression of uncoupled respiration in mitochondria under hypoxia, Proc. Natl. Acad. Sci. U.S. A. 97 (20) (2000) 11080–11085, https://doi.org/10.1073/pnas.97.20.11080.
[63] C. Donnelly, S. Schmitt, C. Cecatto, L.H.D. Cardoso, T. Komlódi, N. Place, B. Kayser, E. Gnaiger, The ABC of hypoxia – what is the norm, Bioenerg Commun 12 (2022), https://doi.org/10.26124/bec:2022-0012.v2, 2022.
[64] R. Liu, P. Jin, L. Yu, Y. Wang, L. Han, T. Shi, X. Li, Impaired mitochondrial dynamics and bioenergetics in diabetic skeletal muscle, PLoS One 9 (3) (2014) e92810, https://doi.org/10.1371/journal.pone.0092810.
[65] L.C. Wollenman, M.R. vander Ploeg, M.L. Miller, Y. Zhang, J.N. Bazil, The effect of respiration buffer composition on mitochondrial metabolism and function, PLoS One 12 (11) (2017) e0187523, https://doi.org/10.1371/journal.pone.0187523.
[66] E.J. Milner-White, D.C. Watts, Inhibition of adenosine 5'-triphosphate-creatine phosphotransferase by substrate-anion complexes. Evidence for the transition-state organization of the catalytic site, Biochem. J. 122 (5) (1971) 727–740, https://doi.org/10.1042/bj1220727.
[67] D.A. Cardinale, K.D. Gejl, N. Ørtenblad, B. Ekblom, E. Blomstrand, F.J. Larsen, Reliability of maximal mitochondrial oxidative phosphorylation in permeabilized fibers from the vastus lateralis employing high-resolution respirometry, Physiological Reports 6 (4) (2018) e13611, https://doi.org/10.14814/phy2.13611.
[68] R.A. Jacobs, C. Lundby, Contextualizing the biological relevance of standardized high-resolution respirometry to assess mitochondrial function in permeabilized human skeletal muscle, Acta Physiol. 231 (4) (2021) e13625, https://doi.org/10.1111/apha.13625.
[69] J.A. Sanford, C.D. Nogiec, M.E. Lindholm, J.N. Adkins, D. Amar, S. Dasari, J. K. Drugan, F.M. Fernández, S. Radom-Aizik, S. Schenk, M.P. Snyder, R.P. Tracy, P. Vanderboom, S. Trappe, M.J. Walsh, C.R. Evans, F.M. Fernandez, Y. Li, L. Tomlinson, M.A. Rivas, Molecular Transducers of physical activity Consortium (MoTrPAC): mapping the dynamic responses to exercise, Cell 181 (7) (2020) 1464–1474, https://doi.org/10.1016/j.cell.2020.06.004.